UNIVERSIDADE FEDERAL DE SANTA MARIA
CENTRO DE CIÊNCIAS NATURAIS E EXATAS
PROGRAMA DE PÓS-GRADUAÇÃO EM CIÊNCIAS BIOLÓGICAS:
BIOQUÍMICA TOXICOLÓGICA

Vinicius Costa Prado

DESENVOLVIMENTO DE UM HIDROGEL DE BASE NANOTECNOLÓGICA CONTENDO UM COMPOSTO DA CLASSE BENZOFUROAZEPINOS COM POTENCIAL FOTOPROTETOR *in vitro*

Santa Maria, RS
2019

Vinicius Costa Prado

DESENVOLVIMENTO DE UM HIDROGEL DE BASE NANOTECNOLÓGICA CONTENDO UM COMPOSTO DA CLASSE BENZOFUROAZEPINOS COM POTENCIAL FOTOPROTETOR *in vitro*

Dissertação apresentada ao curso de Mestrado do Programa de Pós-Graduação em Ciências Biológicas: Bioquímica Toxicológica, da Universidade Federal de Santa Maria (UFSM, RS), como requisito parcial para obtenção do título de **Mestre em Bioquímica Toxicológica.**

Orientador: Prof. Dr. Gilson Rogério Zeni
Coorientadora: Prof.ª. Dr. ª Cristina Wayne Nogueira

Santa Maria, RS
2019

Prado, Vinicius Costa
DESENVOLVIMENTO DE UM HIDROGEL DE BASE NANOTECNOLÓGICA CONTENDO UM COMPOSTO DA CLASSE BENZOFUROAZEPINOS COM POTENCIAL FOTOPROTETOR *in vitro* / Vinicius Costa Prado. - 2019.
63 p.; 30cm

Orientadora: Gilson Rogério Zeni
Coorientadora: Cristina Wayne Nogueira
Dissertação (mestrado) - Universidade Federal de Santa Maria, Centro de Ciências da Saúde, Programa de Pós-Graduação em Ciências Biológicas: Bioquímica Toxicológica, RS, 2019

1. Radiação UV 2. Protetores solares 3. Benzofuroazepinos 4. Nanotecnologia 5. Hidrogel I. Zeni, Gilson Rogério, II. Nogueira, Cristina Wayne, III. Título.

Sistema de geração automática de ficha catalográfica da UFSM. Dados fornecidos pelo autor(a). Sob supervisão da Direção da Divisão de Processos Técnicos da Biblioteca Central. Bibliotecária responsável Paula Schoenfeldt Patta CRB 10/1728.

Vinicius Costa Prado

DESENVOLVIMENTO DE UM HIDROGEL DE BASE NANOTECNOLÓGICA CONTENDO UM COMPOSTO DA CLASSE BENZOFUROAZEPINOS COM POTENCIAL FOTOPROTETOR *in vitro*

Dissertação apresentada ao curso de Mestrado do Programa de Pós-Graduação em Ciências Biológicas: Bioquímica Toxicológica, da Universidade Federal de Santa Maria (UFSM, RS), como requisito parcial para obtenção do título de **Mestre em Bioquímica Toxicológica.**

Aprovado em 26 de julho de 2019:

Gilson Rogério Zeni, Dr. (UFSM)
Presidente, Orientador

Cristina Wayne Nogueira, Dr.ª (UFSM)
Coorientadora

Cristiani Folharini Bortolatto, Dr.ª (UFPEL)

Aline Ourique, Dr.ª (UFN)

Santa Maria, RS
2019

DEDICATÓRIA

Dedico essa Dissertação de Mestrado ao meu avô Marcial Netto *(in memoriam)* como uma singela forma de expressar a minha gratidão aos valores, ensinamentos e suporte que me transferiu até os seus últimos momentos de vida.

AGRADECIMENTOS

Gostaria de, inicialmente, agradecer a Deus e a todos os seres de luz que me acompanham. Gratidão por me concederem saúde, força e garra para eu correr atrás dos meus objetivos e sonhos.
Aos meus pais, Maria Izabel e Ronildo; minhas irmãs Fernanda e Juliana e as minhas avós Ilva e Eloíza. Obrigado pelo amor, suporte e atenção que a mim dedicam. Em especial a minha mãe, por sempre me incentivar a estudar e entender o valor de cada conquista.
Ao meu grupo espiritualista do C.E.U. João Batista: Obrigado pela existência de cada membro desta família unida que somos; "Sozinhos somos fortes, juntos somos invencíveis"!
Aos meus orientadores: Prof.ª Cristina Nogueira (Cris) e Prof. Gilson Zeni (GZ). Cris, muito obrigado pela orientação, ensinamentos e paciência na minha caminhada ao longo destes 5 anos (3 de IC e 2 de mestrado). Sou muito grato pela oportunidade de ter conduzido este projeto. GZ, obrigado pela orientação, preocupação e conselhos nos momentos tensos "no fim vai dar tudo certo jovem"! Agredeço vocês por estarem sempre correndo atrás de melhores condições para a nossa formação.
À Sabrina, "gordines". Mais uma etapa que vamos finalizar juntos! Obrigado por ser esta amiga incrível que tu és. Palavras não são suficientes para descrever a minha gratidão pela amizade, sintonia de pensamentos, e apoio durante o meu recomeço. Desejo a ti, muito sucesso no novo ciclo que vai iniciar e saibas que mesmo não estando perto ficamente por um período, mentalmente estarei. Vou continuar mandando o teu horóscopo todas as segundas-feiras cedão e te deixando em paz pelas manhãs.
A Alessandra e a Karine (Lindosos do CE). Gratidão pelo suporte em momentos delicados e também por dividir momentos maravilhos. Sou uma pessoa privilegiada em ter umas pessoas como vocês por perto.
Ao Marcel, pela amizade, paciência, e tempo dedicado a um aluno que iniciou o mestrado muito imaturo e inseguro. Não tenho palavras suficientes para expressar a gratidão que sinto por você ter plantado e despertado em mim, o gosto pela vida acadêmica e também pela busca incondicional do crescimento em todos os aspectos da vida.
Agradeço ao grupo do Laboratório de Tecnologia Farmacêutica (LabTec)! Muito obrigado por todo conhecimento compartilhado. Agradeço em especial, a prof. ª Letícia Cruz por ter me recebido de braços abertos no seu grupo de pesquisa. Obrigado por te guiado e orientadado o desenvolvimento deste trabalho. Agradeço a Charlene (LabTec) por ter conduzido as análises no Zeta. Obrigado por sempre estar disposta e pelo empenho e capricho nos ensaios.
A Tia Tereza pelo "bom dia guri"! Com certeza, faz e fará muita falta.
A Jéssica (Lab Tec), pelas contribuições e opiniões construtivas no meu trabalho.
Ao Maurício (Lab. Prof. Sérgio) por viabilizar o uso da balança. Foi muito importante a tua contribuição!
Aos meus atuais e ex-colegas do lab Cris e do Lab do GZ pelo compartilhamento diário de conhecimento não só cientifico, mas também de vida. Esse tempo que passamos juntos, foi essencial para o meu aprendizado.
Ao prof. André pelas importantes contribuições na estruturação e desenvolvimento desse trabalho. Agradeço também, a Bruna Cogo. Por todo o empenho, profissionalismo nos ensaios que realizamos.
A Andrezza e a Débora pelo apoio, momentos de diversão e pelo melhor mate da bioquímica.
Ao Maurício, meu amigo de longa data. Obrigado pelo apoio de sempre!
A Fernanda Dias/Noites! Obrigado por sempre estar disposta a me ajudar, a me ouvir, e principalmente por torcer pelo sucesso pessoal e profissional.
A Verônica! A pós-graduação nos aproximou. Sou muito grato a isso. Tu és uma pessoa muito especial! Obrigado pelas contribuições, suporte profissional e memontos de descontração!
A Camila Rampelotto! Por todo o apoio, e por confiar mais em mim que eu mesmo. Obrigado por todas as contribuições, em especial por me ajudar a salvar o HPLC na véspera de Natal!
A Luana Ferreira. Aprendi muito com ela! Minha primeira nano, fiz contigo. Obrigado, pelas dicas e ajudas. Tu és foda!
A minha teacher Annie! Obrigado pelos incentivos e por estar sempre aberta a ouvir meus anseios.
Ao Roberto e a Rafaela pela síntese dos compostos.
A todos os professores do PPGBTOX que contribuíram na minha formação.
A CAPES, pela minha bolsa.
A prof. ª Cristiani e Aline por avaliarem o meu trabalho.

Obrigado.

RESUMO

DESENVOLVIMENTO DE UM HIDROGEL DE BASE NANOTECNOLÓGICA CONTENDO UM COMPOSTO DA CLASSE BENZOFUROAZEPINOS COM POTENCIAL FOTOPROTETOR *in vitro*

AUTOR: Vinicius Costa Prado
ORIENTADOR: Prof. Dr. Gilson Rogério Zeni
COORIENTADORA: Prof.ª. Dr. ª Cristina Wayne Nogueira

A exposição excessiva a uma faixa de luz solar correspondente a faixa UVB (ʎ = 280-320 nm) e UVA (ʎ = 320-400 nm) é a principal causa dos danos na pele humana. Essas alterações são atribuídas a danos em biomoléculas, como lipídeos, proteínas e ao DNA. Atualmente, o uso de protetores solares é considerado a ferramenta mais eficaz para evitar e atenuar os efeitos nocivos da radiação UV na pele. No entanto, essas formulações possuem limitações quanto à sua estabilidade, eficácia e aceitabilidade pelos usuários. Considerando esses aspectos, são necessárias abordagens inovadoras para melhorar a eficácia dos filtros solares, bem como novas moléculas com propriedades de absorção da luz UV. Neste contexto, a classe das benzofuroazepinos possui características estruturais com potencial para a absorção da radiação UV. Além disso, a aplicação da nanotecnologia em formulações fotoprotetoras é promissora porque é capaz de contornar as limitações descritas para esses agentes. Portanto, essa dissertação buscou explorar o potencial de absorção da luz UV de compostos pertencentes à classe dos benzofuroazepinos e, a partir do espectro de absorção, selecionar um composto com o melhor perfil de absorção entre os comprimentos de correspondentes a faixa UVB e UVA. Com o objetivo de selecionar o composto mais promissior, espectros de absorção na faixa UV de três compostos (10µg/mL) foram realizados. Nanocápsulas poliméricas contendo o composto selecionado (3mg/mL) foram desenvolvidas e caracterizadas em termos de tamanho, índice de polidispersão, pH, potencial zeta e conteúdo de composto. Além disso, foi avaliado a toxicidade do composto na sua forma livre ou nanoencapsulada e a influência da nanoencapsulação nas propriedades de absorção/reflexão da luz UV *in vitro*. Posteriormente, um hidrogel contendo as nanocápsulas foi formulado utilizando goma gelana como agente espessante. O potencial fotoprotetor *in vitro* dos hidrogéis foi mensurado pela sua capacidade em atenuar a geração de danos à molécula de DNA exposta a luz UVB e UVA. As suspensões de nanocápsulas contendo o composto selecionado apresentou características físico-químicas apropriadas. Hidrogéis apresentaram valores de pH próximos levemente ácidos, teor de compostos próximo ao valor teórico (3 mg / g), tamanho de partícula na faixa nanométrica e perfil de espalhamento adequado para aplicação cutânea. Todos os hidrogéis contendo o composto selecionado foram eficazes contra a formação de danos a molécula de DNA induzidos pela exposição a fontes de radiação UVB e UVA. Em conclusão, o presente estudo mostrou a identificação de um composto com potencial de absorção da luz UV e a preparação de um hidrogel de base nanotecnológica para a aplicação cutânea.

Palavras chaves: Radiação UV. Protetores solares. Benzofuroazepinos. Nanotecnologia. Hidrogel.

ABSTRACT

DEVELOPMENT OF A NANOTECHNOLOGICAL-BASED HYDROGEL CONTAINING A BENZOFUROAZEPINE COMPOUND WITH PHOTOPROTECTIVE POTENTIAL *in vitro*

AUTHOR: Vinicius Costa Prado
ADVISOR: Prof. Dr. Gilson Rogério Zeni
CO ADVISOR: Prof.ª. Dr. ª Cristina Wayne Nogueira

The excessive exposure to a range of sunlight corresponding to UVB range (ʎ = 280-320 nm) and UVA (ʎ = 320-400 nm) is the main cause of human skin damage. These changes are attributed to damage to biomolecules such as lipids, proteins and DNA. To date, the use of sunscreens is considered the most effective approach to avoid and attenuate the harmful effects of UV radiation on skin. However, the sunscreen formulations have limitations regarding their photostability, effectiveness and safety by users. In this context, benzofuranoazepine class has chemical characteristics with potential for the absorption of UV radiation. In addition, the application of nanotechnology in sunscreens is promising because it is able in modulate the limitations of formulations. Therefore, the aim of this study was to screen benzofuroazepine compound with a broad-spectrum absorption profile in the UVB and UVA ranges. Aiming at selecting the molecule with the highest photoprotective potential the UV absorption spectrum profile of three compounds (10µg/mL) was assessed. Polymeric nanocapsules containing the selected compound (3mg/mL) were developed and characterized in terms of size, polydispersity index, pH, zeta potential and compound content. In addition, the toxicity of the free or nanoencapsulated compound forms and the influence of nanoencapsulation in UV light absorptive/scatter properties of compound were evaluated. In a subsequent step the hydrogels containing nanocapsule suspensions were proposed using gellan gum as a thickening agent. The *in vitro* photoprotective potential of the hydrogels was evaluated by the their ability to attenuate the generation of damages to the DNA molecule exposed to UVB and UVA light. The nanocapsule suspensions containing the selected compound had appropriate physicochemical characteristics (nanometric and homogeneous size distribution) and increased the UV light scattering in comparison to free compound. Hydrogels presented slightly acidic pH values, compound content of 3mg/g in the formulation, particle size in the nanometric range and spreadability profiles suitable to cutaneous application. All hydrogels containing the selected compound were effective against DNA damage induced by the UVB and UVA radiation. In conclusion, the present study showed the identification of a compound with potential for UV light absorption and the preparation of a nanotechnological-based hydrogel for cutaneous application.

Keywords: UV radiation. Sunscreen. Benzofuroazepines. Nanotechnology. Hydrogels.

LISTA DE FIGURAS

INTRODUÇÃO

MANUSCRITO

LISTA DE TABELAS

MANUSCRITO

LISTA DE ABREVIAÇÕES E SIGLAS

(6-4-PPs) – (6-4) pirimidina pirimidona

ANVISA – Agência Nacional de Vigilância Sanitária

COLIPA – *European Cosmetic, Toiletryand Perfumery Association*

CPDs – Ciclobutano de pirimidina

DNA – Ácido desoxirribonucleico

EROs – Espécies Reativas de Oxigênio

FDA – *Food and Drug Administration*

FPS – Fator de Proteção Solar

FP-UVA – Fator de proteção UVA

MMP – Metaloproteinases de matriz

OMS – Organização Mundial de Saúde

UV – Radiação Ultravioleta

SUMÁRIO

1. INTRODUÇÃO

1.1 RADIAÇÃO ULTRAVIOLETA

A faixa de radiação ultravioleta (UV, 100 – 400 nm) corresponde aproximadamente a 7% da radiação eletromagnética emitida pelo sol e conforme a faixa de comprimento de onda pode ser classificada em três categorias: UVC: 100-280 nm; UVB: 280-320 nm e UVA: 320-400 nm (AKHALAYA et al., 2014). A quantidade de radiação UV que chega à superfície terrestre é inferior ao que incide no topo da atmosfera, uma vez que esse tipo de radiação é atenuada em virtude das suas interações com os constituintes da atmosfera como, por exemplo, o oxigênio e a camada de ozônio. Porém, sabe-se que apenas a radiação UVC é totalmente refletida pela camada de ozônio e, consequentemente, não atinge de forma significativa os seres humanos (SCHUCH et al., 2013). Assim, os efeitos biológicos desencadeados pela exposição à radiação UV são atribuídos aos raios UVA e UVB (MOURET et al., 2011). Embora a radiação UV corresponda a uma pequena fração dentro do espectro de radiação solar que incide sobre a superfície terrestre, essa possui efeitos nocivos à saúde humana, sobretudo na pele (NATARAJAN et al., 2014).

1.2 A PELE HUMANA

A pele, uma interface entre os meios externo e interno, desempenha um importante papel na proteção do organismo humano contra agentes nocivos externos, sendo um órgão estruturalmente formado por três camadas: epiderme, derme e hipoderme (STIEFEL; SCHWACK, 2015) **(Figura 1)**. A epiderme é o tecido mais superficial, onde os queratinócitos, principais células constituintes desta porção, estão dispostos em camadas com distintos graus de maturação. Essas células passam por um processo de diferenciação celular que leva à formação da camada mais externa e principal responsável pela proteção contra agentes externos, conhecida como estrato córneo. Por sua vez, a derme é composta por fibroblastos, que são as células responsáveis pela síntese dos componentes estruturais da matriz extracelular (colágeno e elastina), os quais conferem elasticidade, resistência e proteção mecânica ao tecido cutâneo. Nesse contexto, a penetração dos raios UV na pele é guiada pelo seu comprimento de onda, sendo que curtos comprimentos de onda, correspondentes a radiação UVB, atingem somente a epiderme enquanto que os raios UVA, maior comprimento de onda, conseguem atingir a derme (LIEBEL et al., 2012) **(Figura 1)**.

Figura 1 - Organização estrutural da pele e o grau de penetração dos raios UVB e UVA

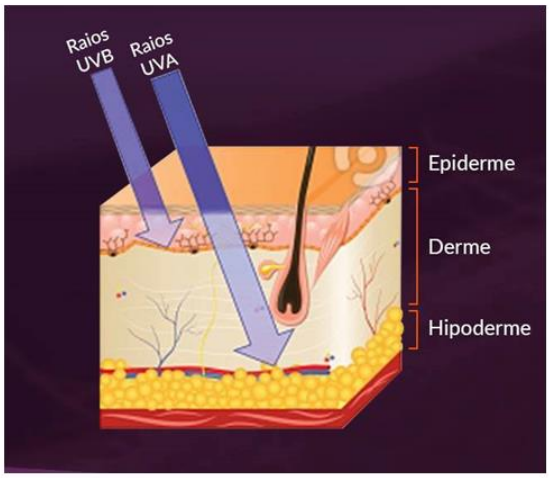

Fonte: Adaptado da Sociedade Brasileira de Dermatologia (2017).

1.3 ALTERAÇÕES BIOQUÍMICAS E MOLECULARES DESENCADEADAS PELA EXPOSIÇÃO À RADIAÇÃO ULTRAVIOLETA

Em nível molecular, os raios UVA e UVB diferem nas suas formas de geração de dano no tecido cutâneo (D'ORAZIO et al., 2013). Ao incidir sobre a pele, a radiação UVB desencadeia eritema (queimaduras solares), imunossupressão, e uma intensa migração leucocitária configurando um quadro inflamatório tecidual (PEGORARO et al., 2017; WANG et al., 2019). Cumulativamente, diversos estudos reportam o expressivo potencial carcinogênico da radiação UVB após repetidas e longas exposições, especialmente pela geração direta de dano ao ácido desoxirribonucleico (DNA) (BAGDE; MONDAL; SINGH, 2018). Corroborando com isso, a literatura científica relata que a exposição à luz UV pode agredir diretamente o DNA, em particular a UVB, a qual desencadeia reações fotoquímicas cutâneas que dão origem a fotoprodutos de DNA, conhecidos como dímeros de pirimidina tais como os ciclobutanos de pirimidina (CPDs) e (6-4) pirimidina pirimidona (6-4-PPs) (SCHUCH et al., 2013, 2017) **(Figura 2)**. Esses produtos são formados a partir da absorção da radiação UVB pela molécula de DNA o que, consequentemente, altera as ligações entre as bases nitrogenadas, gerando assim distorções estruturais na dupla hélice do DNA (MATSUMURA; ANANTHASWAMY, 2004). Essas lesões contribuem para alterações na homeostasia dos processos de replicação e

transcrição celular e, por consequência, favorece processos de mutação celular que estão intimamente implicados com o desenvolvimento do câncer de pele.

Figura 2 - Esquemática representação da geração dos dímeros de pirimidina a partir da exposição da molécula de DNA a luz UV

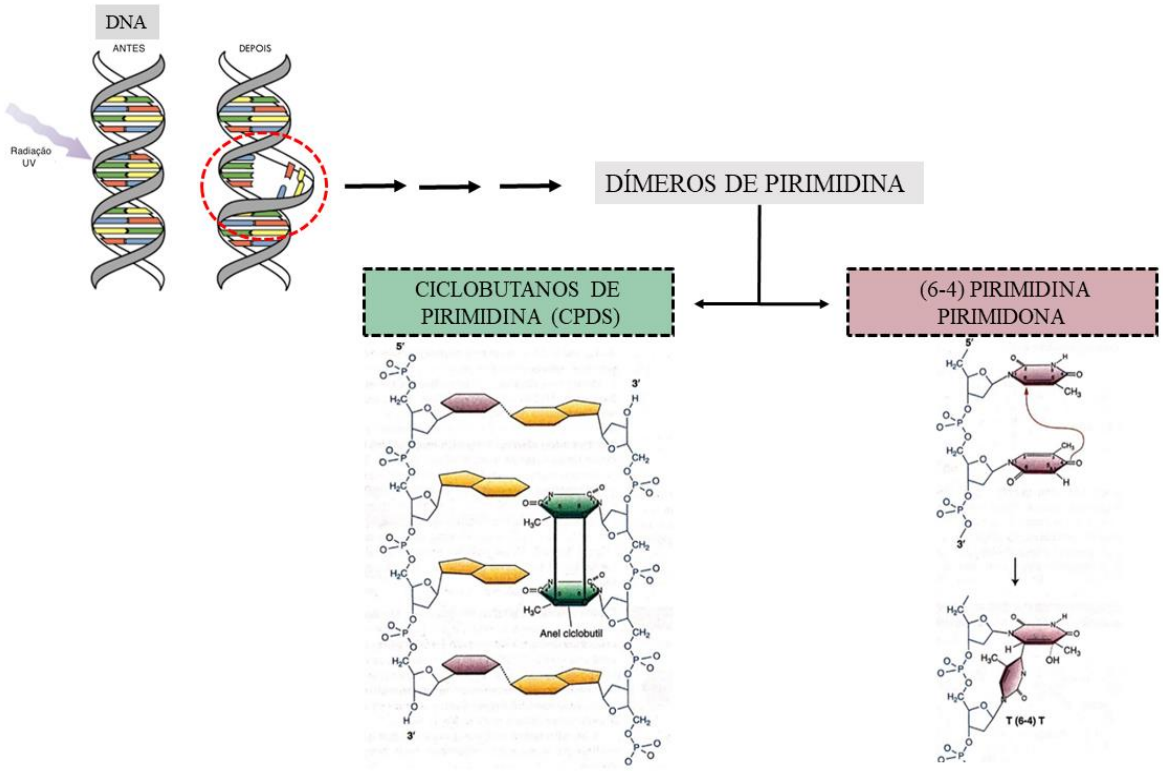

Fonte: O próprio autor.

Por sua vez, os raios UVA são responsáveis por uma intensa geração de espécies reativas de oxigênio (EROs), as quais são formadas a partir da absorção da radiação por substâncias cromóforas presentes no tecido cutâneo como, por exemplo, a melanina e as porfirinas, que uma vez energizadas podem transferir a energia para o oxigênio molecular gerando EROs (NATARAJAN et al., 2014; SCHUCH et al., 2017). Por conseguinte, tem-se a oxidação de macromoléculas como os lipídeos e proteínas celulares, além da ativação de metaloproteinases de matriz (MMP), especificamente as MMP-1, 3 e 9, responsáveis pela degradação do colágeno e de outros constituintes estruturais da pele (QUAN et al., 2009). Em conjunto, estes fatores aceleram o fotoenvelhecimento e são determinantes no desenvolvimento de malignidades do tecido cutâneo (KAMMEYER; LUITEN, 2015). Além disso, embora existam algumas divergências na literatura científica, recentes estudos demonstram que a radiação UVA promove a formação de dímeros de pirimidina pela absorção direta dos raios UVA pela molécula de DNA. Cabe ressaltar que embora a quantidade de absorção seja mínima nos

comprimentos de onda superiores a 320 nm, ela existe especialmente na região UVA I (320 nm – 380 nm) (KUNISADA et al., 2013). Agravando este processo, o percentual de radiação UVA que atinge a superfície terrestre é aproximadamente 20 vezes maior que a radiação UVB (SCHUCH et al., 2017).

Considerando os aspectos abordados anteriormente, o câncer de pele é o tipo de anomalia cutânea mais grave e o que mais desperta preocupação entre as autoridades de saúde pública. Segundo o Instituto Nacional do Câncer (INCA, 2018), no Brasil, o câncer de pele é o tipo de câncer com diagnóstico mais prevalente, chegando a representar 30% dos diagnósticos de neoplasias malignas. Deste modo, a Organização Mundial de Saúde (OMS) orienta a população a adotar medidas de fotoproteção como: evitar exposição ao sol nos períodos com maior incidência de radiação (10 – 16 horas), utilizar vestimentas, óculos e chapéus de proteção e, sobretudo a utilização de protetores solares. Reforçando tais medidas, desde meados dos anos 1980, houve um aumento significativo no nível de radiação UV que atinge a superfície terrestre devido a depleção da camada de ozônio (DAMERIS, 2010).

1.4 FORMULAÇÕES FOTOPROTETORAS

Uma vez conhecidos os danos decorrentes da radiação ultravioleta sobre a pele, o delineamento de formas farmacêuticas com finalidade fotoprotetora representam uma proposta de produtos farmacêuticos de interesse crescente (ZASTROW et al., 2017). Conceitualmente, fotoproteção pode ser definida como uma medida profilática que visa minimizar a exposição aos raios UVA e UVB e, desta forma, atenuar os efeitos nocivos desencadeados pela exposição excessiva ao sol (STENGEL, 2018). Nesse contexto, o uso tópico de protetor solar constitui a medida mais eficiente para proteger a pele dos efeitos prejudiciais dos raios UV e, portanto, a sua utilização é a ferramenta mais efetiva na prevenção do desenvolvimento de neoplasias cutâneas.

De acordo com a Agência Nacional de Vigilância Sanitária (ANVISA), os protetores solares, ou fotoprotetores, são produtos cosméticos classificados como GRAU 2, destinados à aplicação tópica e constituídos por uma combinação de filtros orgânicos e inorgânicos **(Figura 3)**. Os agentes orgânicos, ou filtros químicos, são compostos aromáticos conjugados com um grupo doador de elétrons, que confere a molécula a propriedade de absorver os raios UV em um determinado comprimento de onda, passando para um estado excitado de maior energia e ao retornar para o estado fundamental, de energia inferior, a energia absorvida é dissipada para

a atmosfera (SHAATH, 2010). Como representantes dessa classe, podemos mencionar: os derivados do ácido *para*-aminobenzóico, as benzofenonas, os salicilatos, os cinamatos e outros.

Já os inorgânicos, ou filtros físicos, são substâncias derivadas de metais ou óxido metálicos como, por exemplo, o dióxido de titânio e o óxido de zinco, que atuam como uma barreira física refletindo e dispersando os raios UV. Portanto, para que se obtenha uma proteção eficaz, é necessária uma combinação de diferentes ativos fotoprotetores que, em conjunto, contemplem maior espectro de absorção na faixa UV (YOUNG; CLAVEAU; ROSSI, 2017). De acordo com a legislação vigente no Brasil, a eficácia de uma formulação fotoprotetora é determinada pela avaliação do Fator de Proteção Solar (FPS), do Fator de proteção UVA (FP-UVA) e da avaliação do comprimento de onda crítico, empregando metodologias *in vitro* e *in vivo* reconhecidas pela FDA (*Food and Drug Administration*) e pela COLIPA (*European Cosmetic, Toiletry and Perfumery Association*).

Desta forma, além do apelo cosmético, a formulação fotoprotetora deve apresentar um conjunto de características que, ao ser aplicada na pele, tenha potencial de absorver e dispersar os raios UV de forma efetiva e duradoura (MANCUSO et al., 2017). Logo, almeja-se produtos que sejam quimicamente estáveis e seguros após aplicação e exposição ao sol. Adicionalmente, estes produtos devem apresentar uma baixa permeação cutânea a fim de garantir a residência da formulação nas camadas superiores da pele e, desta forma, minimizar a exposição sistêmica de seus constituintes.

Figura 3 - Classificação dos filtros solares

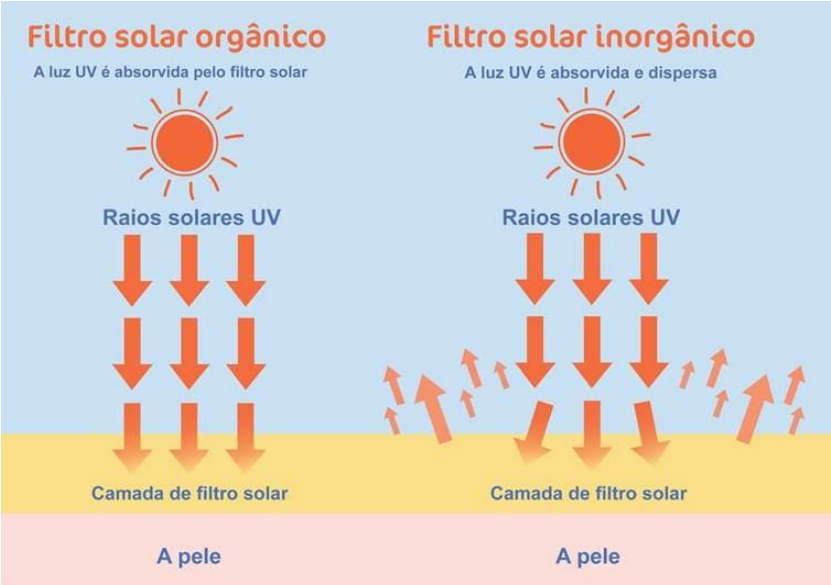

Fonte: Adaptado de Machado et.al., 2011.

1.5 LIMITAÇÕES DOS FOTOPROTETORES SOLARES E O DELINEAMENTO DE NOVAS FORMULAÇÕES

Apesar de efetivos, existem limitações relevantes a serem consideradas na eficácia dos ativos fotoprotetores e também no desenvolvimento farmacotécnico de novas formulações no segmento da fotoproteção. Nesse contexto, a utilização dos óxidos metálicos, como agentes físicos de fotoproteção exibem limitações relacionadas ao aspecto organoléptico e sensorial por dificultar a espalhabilidade e deixar a pele com aspecto esbranquiçado e, desta forma, limita a boa aceitação e adesão pelo consumidor (STIEFEL; SCHWACK, 2015). Adicionalmente, alguns filtros químicos, após absorverem a radiação, sofrem alterações na sua estrutura química ou, até mesmo, geram uma nova molécula, e desta forma acabam perdendo a sua eficácia e potencializando o risco de gerar reações fototóxicas e fotoalérgicas na pele. Este comportamento é denominado de fotoinstabilidade, uma importante limitação atribuída aos filtros químicos utilizados atualmente (STIEFEL; SCHWACK, 2015).

Corroborando com tais limitações, diversos estudos reportam a toxicidade dos ativos fotoprotetores devido à permeação das formulações através das camadas da pele. Ao atingir a derme, um tecido amplamente vascularizado, tem-se a absorção dos ativos e demais constituintes da formulação e, consequentemente uma exposição sistêmica (KRAUSE et al., 2012). Corroborando com isso, vários filtros orgânicos já foram detectados em amostras de urina e de leite materno após a aplicação tópica e, consequentemente, desencadeiam efeitos sistêmicos como desregulações do sistema endócrino (HAYDEN; ROBERTS; BENSON, 1997; KRAUSE et al., 2012). Portanto, novas formulações devem ser propostas visando contornar as fragilidades descritas com os produtos disponíveis no mercado (JOSE; NETTO, 2018; SINGER; KARRER; BERNEBURG, 2019).

Considerando os aspectos abordados, é relevante a pesquisa de novas moléculas com potencial fotoprotetor e que as mesmas atendam a critérios de fotoestabilidade e segurança, além de apresentar amplo espectro de absorção na faixa UV (MANCUSO et al., 2017). Nesse contexto, no nosso grupo de pesquisa, compostos orgânicos de selênio e telúrio são o foco de pesquisas científicas tanto em síntese orgânica, como na aplicação em sistemas biológicos, uma vez que diferentes propriedades farmacológicas têm sido relatadas para estes compostos (NOGUEIRA; ROCHA, 2011; NOGUEIRA; ZENI; ROCHA, 2004). Além disso, moléculas inéditas têm sido sintetizadas em nosso grupo de pesquisa visando incorporar características estruturais importantes para a absorção da luz UV. A classe dos benzofuroazepinos (GAI; BACK; ZENI, 2015) apresenta anéis aromáticos e substituintes que podem potencializar a

absorção dos raios UV e, portanto, podem ser promissores como ativos para integrar uma formulação fotoprotetora. Em vista disso, os compostos 6 – 4 metoxi-5H-benzo [d]benzofuro[3,2b]azepino – (MBBA - **Figura 4A)**, 6- naftaleno-5H-benzo[d] benzofuro[3,2b]azepino – (NBBA - **Figura 4B)** e composto 6-(tiofenil)-5H-benzo[d]benzofuro[3,2b]azepino – (TBBA - **Figura 4C)** são os representantes da classe com características estruturais promissoras para exercerem o papel de filtro UV orgânico. Associado a isso, considerando os recursos tecnológicos disponíveis no âmbito farmacêutico para o desenvolvimento de formulações fotoprotetoras, o emprego da nanotecnologia surge como uma ferramenta capaz de potencializar o fator de proteção solar, agregar o apelo estético, e diminuir a permeação cutânea da formulação fotoprotetora (JIMÉNEZ et al., 2004). Além disso, as nanopartículas possuem a propriedade de reflexão da luz, incluindo os raios UV, salientando que tais formulações podem ser utilizadas como um agente físico de fotoproteção (JOSE; NETTO, 2018).

Figura 4 - Estrutura química dos compostos pertencentes à classe dos benzofuroazepinos

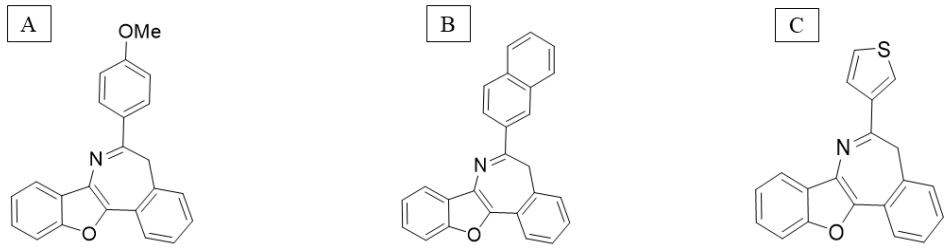

Fonte: Adaptado de Gai et al., 2015.

1.6 SISTEMAS NANOESTRUTURADOS E FOTOPROTEÇÃO

A nanotecnologia é fundamentada na habilidade de caracterizar, manipular e organizar partículas com uma faixa de tamanho de 10 a 1000 nm (KHEZRI; SAEEDI; MALEKI DIZAJ, 2018). Nos últimos anos, a utilização de nanoestruturas para aplicação tópica tem sido o propósito de inúmeros estudos, o que tem contribuído para introdução destes sistemas no mercado farmacêutico e cosmético (GUTERRES; ALVES; POHLMANN, 2007). As nanocápsulas um sistema nanoestruturado de natureza polimérica, são constituídas por um núcleo oleoso envolto por uma matriz polimérica, podendo a substância em estudo estar solubilizada no núcleo, adsorvida a parede da matriz polimérica ou ambos (OLIVEIRA et al.,

2013). Ao entrar em contato com a pele, o perfil de interação e ou permeação cutânea destas nanopartículas depende das suas propriedades físico-químicas, como composição química, tamanho, carga superficial, assim como das propriedades da base dermatológica na qual estão incorporadas. Nesse contexto, a utilização do polímero derivado do ácido metacrílico, Eudragit® RS 100, é uma alternativa para produzir nanoestruturas com superfície catiônica (FRANK et al., 2015, 2018). Ao entrar em contato com o tecido cutâneo, que apresenta carga líquida total negativa, estas nanoestruturas estabelecem interações eletrostáticas que promovem maior permanência no estrato córneo e, deste modo, retarda a permeação cutânea e garante maior eficácia fotoprotetora (CONTRI et al., 2016).

Além da matriz polimérica, o núcleo oleoso da nanoestrutura pode contribuir na ação do sistema, atuando não somente como componente estrutural, mas também exercendo caráter funcional. Nesse contexto, a vitamina E possui inúmeros efeitos benéficos já reportados na literatura quando aplicada no tecido cutâneo, como as atividades antioxidante, anti-inflamatória, fotoprotetora e inibição de dano ao DNA celular em queratinócitos expostos à radiação UV (BROWNLOW et al., 2015; DELINASIOS et al., 2018). Portanto, a utilização de estruturas poliméricas para a nanoencapsulação de filtros solares constitui uma importante escolha para contornar as limitações das formulações convencionais. Porém, cabe ressaltar que, embora as nanocápsulas sejam vantajosas, estes sistemas apresentam-se como suspensões aquosas, o que inviabiliza aplicação no tecido cutâneo (PROW et al., 2011). Logo, a incorporação de nanoestruturas em formulações semissólidas, como os hidrogéis, vem sendo amplamente empregada. Tal alternativa promove uma melhor espalhabilidade sobre a pele e, principalmente, permite a incorporação de substâncias lipofílicas em uma base hidrofílica, minimizando características gordurosas das formulações que não agradam o usuário (MILESI; GUTERRES, 2002). Recentemente, a aplicação da goma gelana como base dermatológica para a produção de hidrogéis foi relatado. Esse semi-sólido foi utilizado para a incorporação de ativos visando sua utilização pela via cutânea, o que tem demonstrado resultados promissores, tanto em termos de características físico-químicas quanto de potencial biológico (MARCHIORI et al., 2017; PEGORARO et al., 2017), reforçando o uso desta matéria-prima.

Portanto, tendo em vista a necessidade do desenvolvimento de formulações com potencial fotoprotetor superior e maior segurança, o presente estudo comprometeu-se a desenvolver, caracterizar e avaliar o potencial fotoprotetor de um hidrogel contendo um composto orgânico na sua forma livre ou nanoencapsulada, visando determinar a influência da nanotecnologia nas características gerais da formulação.

2. OBJETIVOS

2.1 OBJETIVO GERAL

Desenvolver um hidrogel contendo nanocápsulas de um composto orgânico da classe dos benzofuroazepinos visando propor um protetor solar para aplicação cutânea.

2.2 OBJETIVOS ESPECÍFICOS

- Avaliar o espectro de absorção nas faixas UVB e UVA dos três compostos representates da classe dos benzofuroazepinos e, a partir desta análise, selecionar o composto com o melhor perfil de absorção.
- Preparar suspensões de nanocápsulas de Eudragit RS 100® e vitamina E contendo o composto que apresentar o perfil de absorção mais promissor nas regiões UVB e UVA.
- Caracterizar as formulações quanto ao pH, tamanho de partícula, índice de polidispersão, potencial zeta, teor de composto e eficiência de encapsulação.
- Avaliar a fotoestabilidade do composto na sua forma livre e nanoencapsulada em fontes de luz UVA.
- Avaliar a possível toxicidade do composto na sua forma livre ou nanoencapsulada
- Desenvolver um hidrogel contendo nanocápsulas do composto e caracterizar o hidrogel quanto ao teor do composto, pH, espalhabilidade.
- Avaliar o potencial da formulação em proteger o DNA dos danos induzidos pela exposição à radiação UVA e UVB *in vitro*
- Determinar o FPS-DNA *in vitro* do hidrogel contendo o composto na sua forma livre ou nanoencapsulada

3. DESENVOLVIMENTO

O desenvolvimento dessa dissertação está apresentado na forma de um manuscrito em fase de preparação. Os itens introdução, materiais e métodos, resultados, discussão e referências encontram-se descritos no próprio manuscrito.

Development of a nontoxic nanotechnological-based hydrogel containing a novel benzofuroazepine compound with potential photoprotective properties

Vinicius Costa Prado[1]; Marcel Henrique Marcondes Sari[2]; Bruna Cogo Borin[3]; Roberto do Carmo[1]; Letícia Cruz[2]; André Schuch[3]; Cristina Wayne Nogueira[1]; Gilson Zeni*[1]

[1]Laboratório de Síntese, Reatividade e Avaliação Farmacológica e Toxicológica de Organocalcogênios, Centro de Ciências Naturais e Exatas, Departamento de Bioquímica e Biologia Molecular, Universidade Federal de Santa Maria, Santa Maria, CEP 97105-900, RS, Brazil

[2]Laboratório de Tecnologia Farmacêutica, Centro de Ciências da Saúde, Departamento de Farmácia Industrial, Universidade Federal de Santa Maria, Santa Maria, CEP 97105-900, RS, Brazil

[3]Laboratório de Fotobiologia, Centro de Ciências Naturais e Exatas, Departamento de Bioquímica e Biologia Molecular, Universidade Federal de Santa Maria, Santa Maria, CEP 97105-900, RS, Brazil

*Correspondence should be sent to:
Gilson Rogério Zeni
Departamento de Bioquímica e Biologia Molecular, Centro de Ciências Naturais e Exatas, Universidade Federal de Santa Maria, 97105-900, Santa Maria, RS, Brazil.
Phone: 55-55-3220-8140
FAX: 55-55-3220-8978
E-mail: gzeni@ufsm.br

ABSTRACT

The aim of this study was to evaluate the potential DNA photoprotection of nano-based hydrogels containing a novel compound of the benzofuroazepine class. The photoprotective property of three compounds of the benzofuroazepine class were assessed by determining the UV light absorptive profile. Nanocapsule suspensions (Eudragit® RS 100 as polymeric wall and medium chain triglyceride or vitamin E as oil core) containing the compound (3 mg/mL) that had the most uniform spectral absorption in the UVB and UVA ranges were devolpment and characterized (size, polidispersity index, zeta potential, pH, compound content and encapsulation efficiency). The photostability assay, bioadhesive property as well as preliminary toxicity parameters (HET-CAM and *Artemia salina* lethality assays) for free or nanoencapsulated forms of selected compound were also perfomed. In a subsequent step the hydrogels were obtained by thickening nanocapsule suspensions with gellan gum (2%) and characterized concerning of particle size, polydispersity index, pH, compound content and spreadability profile. DNA photoprotection (DNA-SFP) properties of hydrogels were mensured by exposure of DNA samples to the UVB and UVA radiation. Among the tested molecules, the UV absorbance spectrum of free MBBA showed a broad and high intensity absorbance at the UVB and UVA ranges ($\lambda_{\text{MAXIMUM ABSORBANCE}}$ - λ_{MAX}= 290nm). The nanocapsule suspensions containing the selected compound had appropriate physicochemical characteristics (nanometric and homogeneous size distribution), bioadhesiveness property and increased the UV light scattering in comparison to free compound. Besides, all formulations triggered no irritative responses in the HET-CAM test and the nanoencapsulation mitigated the toxic effect to *Artemia salina* observed after the incubation with free form of the compound. Hydrogels showed pH values around acid range, compound content close to the theoretical value (3 mg/g), particle size in nanometric range and spreadability profile suitable for cutaneous application. All hydrogels containing the selected compound were effectivess against the formation of photoproducts, cyclobutane pyrimidine dimers (CPDs) and pyrimidine-6,4-pyrimidinone (6,4PPs) induced by UVB and UVA radiation. In conclusion, the current study showed the identification of a compound with promising UV absorptive potential and the preparation of a final nano-based hydrogel for cutaneous application.

Keywords : UV radiation. DNA damage. Vitamin E. Eudragit® RS 100. Gellan gum. Nano-sunscreens.

1. Introduction

The excessive exposure to the sunlight is the main cause of the skin damages, such as sunburn, photoaging, and skin cancers, which are maining caused by UV light corresponding to UVB (λ=280-320 nm) and UVA (λ=320-400 nm) [1]. These impairments are attributed to cumulative damages in fundamental biomolecules such as deoxyribonucleic acid (DNA), proteins and lipids, causing genome instability and impairments in cellular homeostasis [2]. The potential genotoxicity of the UV radiation is mediated by the formation of covalent bindings with pyrimidine bases, which induces the formation of photoproducts, primarily cyclobutane pyrimidine dimers (CPDs) and pyrimidine-6,4-pyrimidinone photoproduct

(6,4PPs) [3,4]. Cumulatively, these photolesions have negative biological consequences, including mutagenicity, which may lead to cancer of the skin [5,6].

To date, the use of sunscreens is considered the most effective approach to avoid and attenuate harmful effects of UV radiation on the skin [7]. In this context, the UV-filters are compounds incorporated in sunscreen formulations that act absorbing or scattering the UV light. They are classified as either chemical agents (organic UV-filters) or physical agents (inorganic UV-filters) [8]. Chemical UV-filters are aromatic compounds containing series of conjugated π-electron systems on their aromatic rings. The presence of conjugated aromatic rings allows the compound to absorb UV energy [9]. On the other hand, the physical UV-filters are opaque particles that reflect and scatter UV photons [9]. Therefore, an effetive sunscreen formulation is composed of a combination of different UV filters types to provide an uniform broad-spectrum protection against UVA and UVB radiation [10]. Besides that, the formulations should be sensorially adequated and acceptable for the users and high photostable as well [11].

However, the conventional sunscreen formulations have limitations regarding their stability and safety [8,9,12]. In fact, some chemical UV-filters are photochemically unstable, which impair their effectiveness after UV exposure [13]. These filters absorb the UV radiation and reach an excited state and such energy transition can lead the formation of chemically unstable molecules [9]. These products can interact with skin components causing photoallergy and photoxicity reactions [12]. Additionally, the use of physical UV-filters, specifically titanium dioxide and zinc oxide, is limited because of the opaque appearance and occlusive sensation promoted on the skin after the application [14]. Furthermore, a previous study [15], described that the exposure to titanium dioxide induced cytotoxic effects on healthy human keratinocytes, reinforcing the urgent need for novel formulations.

Considereing all these aspects, innovative technologies to improve the efficacy and the safety of sunscreens formulations as well as new molecules with UV light absorptive properties are necessary. In this context, the benzofuranoazepine class has chemical characteristics with potential for the absorption of UV radiation [16]. Similarly to the standard UV filters, the chemical structure of benzofuranoazepine derivative compounds contemplates unsaturated carbon bonds and aromatic rings that may absorb different range of UV light. Futhermore, the application of nanotechnology in sunscreens is a promising approach because it is able to increase the chemical stability of labile compounds and their aesthetic value, improving the solar protection factor (SPF). Nanostructures can also provide superior retention time of substances on the skin surface [17,18], positively contributing to scatter/reflect the UV radiation.

In this sense, polymeric nanocapsules are nanoparticles in which the drug is entrapped in an oily core surrounded by a polymeric wall [19], which can act as physical filter by scatter/reflect the UV light as a consequence of their reduced size range and composition [20]. In addition, the development of nanocapsule suspensions using polymers with mucoadhesive properties for the cutaneous application is an alternative when the aim is to increase the residence time in the stratum corneum [21].

Therefore, the present study proposed the application of the Eudragit RS100®, a cationic polymer with great bioadhesive properties [22], for the development of nanocapsules. Because nanocapsule formulations are obtained as liquid suspensions, a gelling agent is necessary to achieve rheological and spreadability profiles suitable to cutaneous application. Herein, a nano-based hydrogel was obtained using gellan gum, a biocompatible and nontoxic microbial polysaccharide. Previous studies demonstrated the feasibility of preparing hydrogel formulations containing nanocarriers-loaded active substances by a simple and low-cost methodology [23,24].

Thus, the first aim of this study was to screen benzofuroazepine compound with a broad-spectrum absorption profile in the UVB and UVA ranges. The second objective was to develop a nontoxic nanotechnological-based hydrogel containing a novel benzofuroazepine compound with potential photoprotective properties.

2. Materials and methods

2.1 Drugs and reagentes

The following benzofuroazepine compounds were tested in our study: 6(Naphthalen)-5H-benzo[d]benzofuro[3,2-b]azepine - NBBA; 6-(thiophen-3-yl)-5H-benzo[d]benzofuro[3,2-b]azepine - TBBA and the 6-(4-methoxyphenyl)-5H-benzo[d]benzofuro[3,2-b]azepine – MBBA **(Supplementary material: Figures 1AS, 1BS and 1CS respectively)**. The molecules were synthesized following a previous described method [16]. The Eudragit RS100®, polysorbate 80 (Tween® 80) and medium chain triglycerides (MCT) were provided by Delaware (Porto Alegre, Brazil). The sorbitan monooleate (Span® 80) was obtained from Sigma Aldrich (Brazil). The vitamin E acetate (VIT E) was obtained from Mapric (São Paulo, Brazil). The methanol, ethanol, acetone, dimethylsulphoxide (DMSO) were obtained from Tedia (São Paulo, Brazil). All other reagents and solvents were of analytical grade and used as received.

2.2 Pre-formulation studies

2.2.1 Screening of the compounds: UV absorption spectrum

Aiming at selecting the molecule with the highest photoprotective potential the UV light absorptive profile was assessed using an UV-spectrophotometer. The compounds were separately dissolved in ethanol (10 µg/mL) and an aliquot of each solution was placed in a quartz cuvette (model 106-QS, Hellma, Germany) to the UV absorbance scan (ʎ= 280 – 320 nm corresponding to UVB range and 320 – 400 nm corresponding to UVA range). For comparison purposes, the reference UV filters (*p*-aminobenzoic acid - PABA and benzophenone 3 - BZ3) were evaluated in the same experimental conditions. Figure 1S shows the chemical structure of each compound and their respective UV absorption spectra are available in the **(Supplementary material Figures 1AS, 1BS and 1CS)**.

The compound 6-(4-methoxyphenyl)-5H-benzo[d]benzofuro[3,2-b]azepine –MBBA; **(Supplementary material: Figure 1CS)** showed an uniform spectral absorption profile in the UVB and UVA regions. Besides that, MBBA demonstrated superior absorption signals in the UVA and UVB spectra when compared to the other compounds of benzofuroazepine class tested. Based on these results, we selected the MBBA to the further steps of our study.

The ^{1}H and ^{13}C nuclear magnetic resonance (^{1}H-NMR; ^{13}C-NMR) spectra of analysis of the MBBA **(Supplementary material – Figure 2AS and Figure 2BS respectively)** showed analytical and spectroscopic data in full agreement with its assigned structure.

2.2.2 Dissolution/swelling testing

In order to evaluate the compatibility between the polymer, the component of nanocapsules wall, and VIT E, the oil core, we performed the assay of dissolution/swelling of Eudragit RS100® films. The films were prepared by previous dissolving the polymer in chloroform. After solvent evaporation, the films were completely immersed in the VIT E, which were stored in amber glass flasks at room temperature (n=3). Over a 60-day experimental period, the weight of the films was monitored by removing them from the contact with the VIT E and drying with an absorbing paper. The analytical balance was used to determine the weight variation of polymer films. The results were expressed as percentage (%) of weight variation of polymer films.

2.2.3 Analytical method for the MBBA quantification

The MBBA compound was quantified by the high-performance liquid chromatography method: UV detection (HPLC-UV) (Shimadzu, Japan, LC-10A system) equipped with a LC-20AT pump, an UV-VIS SPD-M20A detector, a CBM-20A system controller and a SIL-20A HT autosampler valve. The column used was a C18 (Phenomenex Gemini reversed phase, 5 μm, 110 Å, 150 mm x 4.60 mm). The mobile phase used consisted of an isocratic system (10% of ultrapure water and 90% of methanol) at a flow rate of 1.0 mL/min. The volume of injection was 20 μL and the amount of MBBA in the samples was determined at 208 nm with retention time of 6.5 min. The methodology was linear (r=0.99), specific (96.2 to 103.5 %) and precise (relative standard deviation ≤ 1.61 %) in a concentration range of the 5.0 - 25.0 μg/mL. The method for the MBBA quantification was validated in agreement with the International Conference on Harmonization (ICH) guidelines.

2.3 Preparation and physicochemical characterization of MBBA-loaded nanocapsule suspensions

2.3.1 Preparation of MBBA-loaded nanocapsule suspensions

The nanocapsule suspensions were produced by the interfacial deposition of preformed polymer method. The **Table 1** depicts the qualitative and quantitative composition of each formulation. An organic phase composed of MBBA, Eudragit RS100® polymer, VIT E or MCT oil, Span® 80, and acetone was kept under moderate magnetic stirring at 40°C during 1 h. After the complete dissolution of the components, this phase was injected into an aqueous phase (Tween® 80 and ultrapure water) and maintained under magnetic stirring at room temperature. After 10 min, the solvents were eliminated and the suspension was concentrated under reduced pressure (Rotary evaporator R 114, Büchi®) until the final volume of 10 mL, which corresponds to the a MBBA concentration of 3 mg/mL ($NC_{MBBA\text{-}VIT\ E}$ or $NC_{MBBA\text{-}MTC}$). For comparison purposes, formulations without MBBA ($NC_{B\text{-}VIT\ E}$ and $NC_{B\text{-}MCT}$ – blank nanocapsule suspensions) were also prepared. Three batches of each formulation were prepared and stored in glass containers at room temperature (25ºC).

2.3.2 Physicochemical characterization of MBBA-loaded nanocapsule suspensions

2.3.2.1 Particle size, polydispersity index (PDI) and zeta potential

The particle size (z-average hydrodynamic diameter) and polydispersity index were evaluated using ZetaSizer® Nano Series Malvern Instruments (UK), by the photon correlation spectroscopy method, after diluting samples in the ultrapure water (1:500). The zeta potential was determined by microelectrophoresis using the same equipment, after diluting samples in 10 mM NaCl (1:500). In addition, the volume-weighted mean diameters D[4:3] and SPAN were determined by laser diffraction (Mastersizer 2000®, Malvern Instruments, UK). The samples were directly added to distilled water in the dispersion unit of the equipment until reaching the adequate obscuration index (10 - 12%). The refractive index of the polymer (1.38) was used for the analysis. The SPAN values, which represent the polydispersity of the nanocapsules suspensions, were determined according to the equation (1):

$$\text{SPAN} = d(0.9) - d(0.1) \,/\, d(0.5) \quad (1)$$

where d(0.9), d(0.1) and d(0.5) are the diameters at 90%, 10%, and 50% of the cumulative distribution of the diameter curve, respectively.

2.3.2.2 MBBA content and encapsulation efficiency

The MBBA content in the nanocapsule suspensions was determined by the HPLC method described in the section 2.2.3. An aliquot of 50 µL of nanocapsule suspensions was diluted in 10 mL of methanol, sonicated for 10 min, filtered through a 0.45 µm membrane and injected into the HPLC system. In order to determine the encapsulation efficiency (EE%), an aliquot of the formulation was placed in a 10.000 MW centrifugal device (Amicon® Ultra, Millipore) and the free compound was separated by ultrafiltration/centrifugation technique (10 min at 2200 g). The difference between total and free MBBA concentrations, determined in the nanocapsule and in the ultrafiltrate, respectively, was defined as nanocapsules EE%.

2.3.2.3 pH

The pH of each formulation was measured using a potentiometer (Model pH 21, Hanna Instruments, Brazil). A previously calibrated electrode was immersed in the nanocapsule suspension to determine the pH values.

2.3.2.4 Stability evaluation

The nanocapsule suspensions were packaged in the amber glass flasks and stored at room temperature. After 15, 30 and 60 days, the following parameters were assessed: average diameter, PDI, zeta potential, pH and the MBBA content in the nanocapsules suspensions, which were evaluated as previously described in previous sections.

2.4 Photostability evaluation

The photostability study (n=3) was performed using a mirrored chamber (1 m x 25 cm x 25 cm) coupled with an ultraviolet lamp (Phillips TUV lamp–UVA long life, 30 W), which emits ultraviolet radiation A. The aliquots of the free MBBA (methanol) or MBBA-loaded nanocapsule suspensions ($NC_{MBBA\text{-}VIT\ E}$ or $NC_{MBBA\text{-}MTC}$) were individually placed in plastic cuvettes with covers and exposed to the UVA radiation during 8 h. After this period, the MBBA content was determined by the HPLC method as described in the section 2.2.3. The dark control (plastic cuvette containing MBBA methanolic solution protected from radiation with aluminum paper) was also evaluated, in order to discard degradation by temperature or the influence of other experimental conditions. The results were expressed as % of remaining compound.

2.5 *In vitro* UV light absorptive/scatter properties of the nanocapsule suspensions

The MBBA-loaded nanocapsule suspensions were scanned under the UV light (λ= 280 – 320 nm (UVB range) and 320 – 400 nm (UVA range)) using an UV-spectrophotometer. The formulations were diluted in ultrapure water to achieve the desired concentration (10 µg/mL) MBBA ($NC_{MBBA\text{-}VIT\ E}$ or $NC_{MBBA\text{-}MTC}$). Blank formulations were also tested in the same conditions ($NC_{B\text{-}VIT\ E}$ and $NC_{B\text{-}MCT}$). The samples were added in a quartz cuvette (model 106-QS, Hellma, Germany) for the analyses. The experiments were conducted in triplicate for each concentration.

2.6 *In vitro* bioadhesiveness assay: Interactions between MBBA-loaded nanocapsules and mucin

The mucoadhesive properties of the MBBA-loaded nanocapsules were evaluated using mucin from porcine (type II) [25]. The mean particle size and zeta potential before and after contact with mucin were measured to determine the ability of nanocapsules to interact with the mucin. The nanocapsule suspensions (n = 3/formulation) were diluted into mucin dispersion (1:500 v/v) to determine, by ZetaSizer®, the mean particle size and zeta potential. The mucin dispersion was prepared in ultrapure water at 0.1%. The mean particle size and zeta potential were expressed before and after mucin contact.

2.7 Preliminary toxicity assessment of MBBA-loaded nanocapsule suspensions

2.7.1 Evaluation of irritant potential by chorioallantoic membrane

In order to evaluate the irritation potential of the free- or encapsulated-MBBA, we used the test of chorioallantoic membrane (HET-CAM) [26]. For the assay, fertilized chicken eggs with 10 days of incubation (37 °C and 65% relative humidity) were used. After this period, the most external shell and the white membrane were removed and 300 μL of the formulations were applied onto the chorioallantoic membrane (CAM) (n = 6/formulation). After 20 s, the samples were washed with saline solution and the CAM was monitored until 300s. During this period, any modification in the membrane was monitored (vasoconstriction, hemorrhage and coagulation) and the time need to occur such phenomena was recorded. The MBBA-loaded nanocapsules ($NC_{MBBA\text{-}VIT\ E}$ or $NC_{MBBA\text{-}MTC}$) were compared to the free compound form (dispersion in aqueous solution with 10% of Tween® 80 and 10% of DMSO). In order to verify if the formulation constituents cause any irritating effect, we tested blank nanocapsule suspensions ($NC_{B\text{-}VIT\ E}$ and $NC_{B\text{-}MCT}$), and positive (0.1 N sodium hydroxide - NaOH and 1% sodium lauryl sulfate - SLS) and negative (saline solution) controls. The irritation score (IS) was determined according to the equation (2):

$$IS = [(301 - Time_H)/300] \times 5 + [(301 - Time_L)/300] \times 7 + [(301 - Time_C)/300] \times 9 \quad (2)$$

Where, h = hemorrhage time; v = vasoconstriction time and c = coagulation time. From the IS values obtained, the lesions were classified as non-irritant (0 – 0.9); slightly (1 – 4.9); moderate (5 - 8.9) and severe irritant (9 – 21).

2.7.2 *In vivo* toxicity study - *Artemia salina* as an alternative toxicological method

To investigate whether free or nanoencapsulated MBBA form triggers any acute toxic effect, the *Artemia salina* lethality assay was performed according to previously described method [27]. In this assay, *A. salina* cysts were placed in a bottle containing an artificial sea water prepared by the mix of marine sodium (35g) and sodium bicarbonate (1g) diluted in 1 L of distilled water. After 24 h of incubation at 30°C under conditions of strong aeration and continuous illumination, the *A. salina* reached the larvae in the first stage (*Nauplii*). Glass tubes containing ten larvae were incubated with the free MBBA form or this compound incorporated into the NC ($NC_{MBBA\text{-}VIT\ E}$ or $NC_{MBBA\text{-}MTC}$) at concentrations 2.5, 5, 10, 15, 25 and 50 µg/mL. The blank formulations were tested following the same experimental conditions (concentration and time of incubation). The larvae were also incubated with the vehicles (DMSO – vehicle of the free MBBA) and (ultrapure water - vehicle for the nanocapsule suspensions). The experiments were conducted in triplicate for each concentration. After 24 h of incubation the survival rate (%) of the larvae was indicated by normal locomotion such as visible movement. The lethal concentration (LC50) was calculated.

2.8 Preparation and physicochemical characterization of hydrogels containing the MBBA-loaded nanocapsule suspensions

2.8.1 Preparation of hydrogels

Hydrogels containing the MBBA-loaded nanocapsule suspensions ($HG\text{-}NC_{MBBA\text{-}VIT\ E}$ and $HG\text{-}NC_{MBBA\text{-}MCT}$) and their respective unloaded (blank) formulations ($HG\text{–}NC_{B\text{-}VIT\ E}$ and $HG\text{-}NC_{B\text{-}MCT}$) were obtained by thickening nanocapsules suspensions with gellan gum at 2%, according to a previously described method [24]. For the hydrogel containing the non-encapsulated MBBA ($HG\text{-}_{FREE\text{-}MBBA}$), the compound was solubilized in DMSO (10%) and incorporated into a hydrogel previously prepared in ultrapure water and gellan gum. A final compound content of 3 mg/g of hydrogel was obtained. In addition, the hydrogel vehicle ($HG\text{-}_{VEHICLE}$) was prepared following the same conditions, dispersing 2% of the gellan gum in

ultrapure water. After preparing, 0.5% imidazolidinyl urea was added in the hydrogels. Three batches of each formulation were prepared and stored in plastic container and stored at room temperature.

2.8.2 Physicochemical characterization of hydrogels

2.8.2.1 Mean particle size, polydispersity index (PDI)

The mean particle size and PDI of the nanocapsules incoporated in the hydrogels were measured using ZetaSizer®, by photon correlation spectroscopy method after dispersing the samples in ultrapure water (1:500).

2.8.2.2 pH

The pH values of hydrogels were determined by the immersion of a calibrated potentiometer (Model pH 21, Hanna Instruments, Brazil) in a dispersion of each formulation in ultrapure water (10% w/v).

2.8.2.3 MBBA content in hydrogels

The MBBA content of the hydrogels was determined by HPLC according to the method described in the section 2.2.3. A predetermined amount of each hydrogel was placed in the volumetric flask and the compound extraction was proceded by adding methanol and using an ultrasound bath (30 min). Following, the HPLC analyses were carried out out in filtered samples.

2.8.2.4 Spreadability factor

The spreadability was evaluated according to the methodology described by Rigo and co-workers [28]. The sample was placed in a central hole (1 cm diameter) of a mold glass plate that was positioned on a scanner surface (HP Officejet, model 4500 Desktop). The mold plate was removed and the sample was subsequently pressed with glass plates of known weights, in intervals of 1 min between each plate. The spreading area images were captured at each 1 min interval employing the desktop scanner. The software ImageJ (Version

1.49q, National Institutes of Health, USA) was used to calculate the captured image areas. The spreadability factor (Sf), the spreading capacity on a smooth horizontal surface when one gram of weight is added to it, was calculated following equation (3):

$$Sf = A / W \quad (3)$$

Where, Sf is the spreadability factor (mm^2/g), A is the maximum spread area (mm^2) after addition of the total number of plates and W is the total weight added (g).

2.9 *In vitro* photoprotection assay of hydrogels containing the MBBA-loaded nanocapsule suspensions

2.9.1 DNA photoprotection properties

2.9.1.1 Plasmid extraction

The plasmid DNA samples (pCMUT vector, 1762 bp) were purified using the Qiagen Plasmid Maxi Kit (Valencia, CA) with freshly transformed *Escherichia coli* strain DH10b [29]. After, the samples were stored in a buffer (10 mM Tris-HCl [pH 8.0], 1 mM ethylenediaminetetraacetic acid (EDTA)) at -20ºC prior to the initiation of experiments.

2.9.1.2 Exposure of DNA to the UVB and UVA radiation: The DNA dosimeter system

The DNA dosimeter apparatus was produced using a special frame developed with the Elastomer Syslgard 184 Kit (Dow Corning Corporation, Midland, MI). The DNA samples were applied in triplicate inside the prototype for the desired exposure times. Before the irradiation, the hydrogels ($HG\text{-}_{FREE}MBBA$, $HG\text{-}NC_{MBBA\text{-}MCT}$ or $HG\text{-}NC_{MBBA\text{-}VIT\ E}$) were homogeneously spread onto the surface of the biosensor with a fine brush at a density of 2 mg/cm^2 following the recommendations from the *European Cosmetic, Toiletry and Perfumery Association* (COLIPA) International Sun Protection Factor (SPF) test method guideline. The DNA dosimeters were exposed to the UVA radiation (300 kJ/m^2 - UVA lamp (FDA KY10s, Osram Ultramed, Germany) or UVB radiation (75 kJ/m^2 - UVB lamp (T15M, Vilber Lourmat, France) [3] in the presence or absence of hydrogels.

2.9.1.3 DNA photoproduct quantification, percentage of the DNA photoprotection and the sun protection factor for the DNA (DNA-SPF) of hydrogels.

After separation by 0.8% agarose gel electrophoresis, the relative amounts of supercoiled and open-circular relaxed plasmid DNA were measured by densitometry analysis (ImageQuant - GE Healthcare, Little Chalfont, UK). Samples with 300 ng of DNA were pre-incubated with 0.8 U of Formamidopyrimidine DNA Glycosylase (Fpg: recognizes oxidatively generated damage in purines), 1 U of Endonuclease III (recognizes oxidized pyrimidines and AP sites) and 70 ng of T4-endonuclease V (T4 bacteriophage endonuclease: specific for CPDs) prior to the identification of different DNA lesions. The samples were then incubated at 37ºC for 60 min. The number of enzyme-sensitive sites of damage per kbp of plasmid DNA was calculated, assuming Poisson distribution that was adapted for this technique, by the following equation (4):

$$X= -\ln(1.4 \times FI/(1.4 \times FI + FII))/1.8 \quad (4)$$

where, FI represents the intensity of fluorescence measured in the supercoiled DNA bands, FII represents the intensity in the open-circular relaxed DNA bands, 1.4 is a correction factor to account for the increased fluorescence of ethidium bromide when this compound is bound to relaxed DNA compared to supercoiled DNA, and 1.8 is pCMUT vector size in Kbp [30]. The quantity of DNA lesions calculated for the irradiated DNA samples were subtracted from the number of breaks observed in the non-irradiated control samples and the results were expressed in terms of the DNA breaks/kbp. In addition, the individual percentage of DNA photoprotection of hydrogels was determined as the arithmetic average of the percentages of protection for both CPDs (CPD photoprotection) and oxidized DNA bases (oxidized DNA bases photoprotection) in each irradiated DNA sample.

The calculation of DNA-SPF, adapted from the COLIPA International Sun Protection Factor (SPF), was determined as the arithmetical mean of the individual DNA-SPF (DNA-SPFi) values obtained from the total number (n) of UV irradiations by the following equation (5):

$$\text{DNA-SPF}= (\sum \text{DNA} - \text{SPF}_i)/n \quad (5)$$

Where, the DNA-SPFi is calculated by the ratio between the total amount of DNA lesions (CPDs + oxidized DNA bases) induced by the UV light in each DNA sample without hydrogels and the total amount of DNA damage verified in each irradiated sample in the presence of hydrogel ($HG\text{-}_{FREE\text{-}MBBA}$, $HG\text{-}NC_{MBBA\text{-}MCT}$ or $HG\text{-}NC_{MBBA\text{-}VIT\ E}$).

2.10 Statistical evaluation

The results were expressed as mean ± mean standard error (S.E.M.) and the data normality was evaluated by the D'Agostino and Pearson omnibus normality test. The GraphPad Prism® version 7 software was used to perform the Student's t test and the variance analyses one-way or two-way (ANOVA) followed by the post-hoc Tukey's test. Values of $p<0.05$ were considered statistically significant.

3. Results

3.1 MBBA, similar to standard UV filters, absorbed at UVA/UVB range spectrum

The representative UV absorbance spectrum of free MBBA showed a broad and high intensity absorbance at the UVB and UVA ranges ($\lambda_{MAXIMUM\ ABSORBANCE}$ - $\lambda_{MAX=}$ 290nm) (**Figure 1**). As expected, the representative UV spectrum of PABA ($\lambda_{MAX=}$ 290nm) and BZ3 ($\lambda_{MAX=}$ 290nm) also depicted a profile of absorbance in the wavelength tested **(Figure 1).**

3.2 VIT E did not cause dissolution/swelling of the Eudragit RS100® films

The compatibility between Eudragit RS 100® and VIT E was evaluated by monitoring the weight change of polymer films. After 60 days of experiment, the weight of films showed a slight increase of the 1.65 %, suggesting no significant swelling/dissolution of polymer films over the experimental evaluation.

3.3 MBBA-loaded nanocapsule suspensions had appropriate physicochemical characteristcs and stability

The results of organoleptic analysis showed that the nanocapsule suspensions were odorless and opaque. The formulations were macroscopically homogeneous and had nonvisible

precipitation. The MBBA-loaded nanocapsules and blank nanocapsule suspensions showed the mean particle size of about 175 nm with a narrow size distribution, which is represented by a PDI value < 0.150 **(Table 2)**. Corroborating with these data, laser light diffraction analysis demonstrated nanoparticles with a narrow size distribution and excluded the presence of microparticles **(Table 3)**. In addition, all formulations had positive zeta potential and a slightly acidic pH **(Table 2)**. The encapsulation efficiency of MBBA was around 100% as well as the drug content in the formulation, which was around 100 % to both VIT E and MCT composed nanocarriers **(Table 2)**. The statistical analysis performed by One-way ANOVA (day 0) revealed no significant differences among the formulations to all tested parameters (p>0.05). Regarding the statistical analysis, the oil type did not have any influence on the physicochemical characteristcs of formulations.

After 15, 30 and 60 days of storage at room temperature, the formulations showed the same macroscopic appearance without any visible alterations. In addition, no statistical difference was found to any physicochemical parameter tested (size, PDI, and pH) when compared to day 0 (p>0.05 Two-way ANOVA of repeated measures) **(Supplementary Material: Figures 3AS, 3BS and 3CS respectively)**. However, the zeta potential values **(Supplementary Material: Figure 3CS)** showed an increased for both formulations on 15, 30 and 60 days in comparasion to day 0 (p<0.05; Two-way ANOVA of repeated measures followed by the Tukey's test). In adition, there was a decrease of drug content (%) for both MBBA-loaded nanocapsules (MCT and VIT E) on days 30 and 60 **(Supplementary Material: Figure 3ES)** (p<0.05; Student’s t test paired followed by the Tukey's test).

3.4 Free or nanoencapsulated MBBA forms are photostable

After 8h of the UVA light exposure, no statistically significant changes in the MBBA remaining concentration (%) were found to free (Free MBBA = 100.3±1.9; dark control = 99.1±0.9) or MBBA-nanoencapsulated forms ($NC_{MBBA\text{-}VIT\ E}$ = 97.0±10.8; $NC_{MBBA\text{-}MTC}$ = 98.3±1.5) (p>0.05; One-way ANOVA).

3.5 MBBA-loaded nanocapsule suspensions are effective in scatter/absorb the UV light

After UV scanning, the results of spectra showed that MBBA-loaded nanocapsule suspensions were effective to scatter/absorb the UV light. The aqueous dispersion of $NC_{MBBA\text{-}VIT\ E}$ had a broad spectrum of absorption at the UVB and UVA regions **(Figure 2A)** with

maximum intensity at the UVB region ($\lambda_{MAX=}$ 290nm). The spectrum of $NC_{MBBA-MTC}$ **(Figure 2B)** presented a similar pattern, but with lower intensity of scatter/absorb ($\lambda_{MAX=}$ 290nm). In addition, the UV spectrum of aqueous dispersion of the $NC_{B-VIT\ E}$ **(Supplementary Material: Figure 4AS)** and NC_{B-MCT} **(Supplementary Material: Figure 4BS)** showed a profile of UV absorption in the wavelength range tested but in lower intensity profile in comparison to the formulations containing MBBA-encapsulated ($\lambda_{MAX=}$ 280nm; $\lambda_{MAX=}$ 280nm respectively).

3.6 MBBA-loaded nanocapsules had bioadhesiveness properties

Figure 3A and **Figure 3B** show the mean particle size and zeta potential of the MBBA-loaded nanocapsules ($NC_{MBBA-VIT\ E}$ or $NC_{MBBA-MTC}$) and their respective unloaded (blank) formulations ($NC_{B-VIT\ E}$ and NC_{B-MCT}) before and after interaction with the mucin dispersion. After the exposure to mucin there was a statistically significant increase of mean particle size when compared to the initial measure ($p<0.05$; Two-way ANOVA followed by Tukey's test). In addition, the zeta potential values changed from positive to negative charge, indicating an interaction between particles and mucin ($p<0.05$; Two-way ANOVA followed by the Tukey's test).

3.7 MBBA-loaded nanocapsule suspensions did not cause irritant effect on the CAM

The **Figure 4** shows representative imagens of the CAM after the assay. MBBA-loaded nanocapsules (IS = 0), blank nanocapsules (IS = 0), and free MBBA (IS=0) showed no irritant effect after their application in the CAM. As expected, the positive controls were classified as severe irritants (IS = 16.4 ± 1.2 to the 1% SLS and IS = 10.4 ± 0.2 to the 0.1 N NaOH). No irritant reactions in the CAM were found to the negative control (saline solution) (IS=0).

3.8 MBBA-loaded nanocapsules suspensions did not decrease the % survival rate of the *Artemia salina*

The **Table 4** shows the media of % survival rate of the *Artemia salina* larvae exposed to the MBBA free or nanoencapsulated form. After 24 h of incubation, the free MBBA form decreased the % of survival rate larvae to 70, 50 and 0 % at 15 µg/mL, 25 µg/mL and 50 µg/mL concentrations, respectively (LC_{50}= 19.8 µg/mL), suggesting acute toxicity. By contrast, both formulations containing MBBA-loaded nanocapsules ($NC_{MBBA-VIT\ E}$ or $NC_{MBBA-MTC}$) and their

respective unloaded (blank) formulations ($NC_{B\text{-}VIT\ E}$ and $NC_{B\text{-}MCT}$) did not reduce the % of survival rate of the larvae at any concentration tested (LC_{50} > 50 µg/mL).

3.9 Physicochemical characterization of hydrogels

Table 5 demonstrates the detailed physicochemical characteristics of the hydrogels. The mean diameter of nanocapsules incorporated in hydrogels showed nanometric size, similarly to the original suspension. Corroborating with such data, all formulations had slightly acid pH values and PDI <0.22, indicating a narrow particle size distribution. The MBBA content in the hydrogels containing the compound was around 100%, resulting in a compound content of 3mg/g in the formulation. The spreadability factor values were similar for all hydrogels. In addition, all formulations were macroscopically homogeneous and have opalescent appearance. The statistical analysis performed by One-way ANOVA revealed no significant difference among the formulations to all tested parameters (p>0.05).

3.10 MBBA nanotechnological-based hydrogel protected against DNA damage induced by UV radiation exposure

Figure 5A demonstrates the representative images of the electrophoretic migration in agarose gels for distinguish supercoiled DNA (form I – FI (first band); free from UV-induced DNA damage) from open-circular relaxed DNA that contained breaks caused by enzymatic cleavage after recognition of the specific UV-induced DNA damage (form II – FII (second band)).

The quantification of the DNA breaks (DNA from II - FII) induced by exposure of DNA to UVB **(Figure 5B)** or UVA **(Figure 5C)** radiation revealed a significant increase of CPDs formation (by T4 enzyme) when compared with the control (non-irradiated DNA samples). All hydrogels containing the compound ($HG\text{-}_{FREE\text{-}MBBA}$, $HG\text{-}NC_{MBBA\text{-}MCT}$ or $HG\text{-}NC_{MBBA\text{-}VIT\ E}$) were effective against the increase of the CPDs formation induced by the UVB and UVA radiation. Regarding oxidized DNA damage (by fpg enzyme), the exposure to UVA **(Figure 5B)** and UVB **(Figure 5C)** did not induce a significant increase in this parameter when compared to CPDs formation. Corroborating with these data, DNA-SPF values as well as the percentage of DNA photoprotection are ilustrated in **Table 6**. Although the DNA-SPFs were lower than traditional SPFs values of the comercial sunscreens, all hydrogels containing the

compound showed satisfactory protection against the genotoxic impact induced by exposure to UVB and UVA radiations.

4. Discussion

The issues related to sunscreen formulations usage motivated the development of products with improved efficacy. Herein, a nano-based hydrogel with photoprotective properties was obtained by incorporating a high UV-absorptive molecule into nanocapsules. The results demonstrated that the MBBA nanoencapsulation positively impacted its photoprotective effect. Besides, the formulation is physicochemically stable, showed no *in vitro* toxicity (HET-CAM test and *Artemia salina*) and prevented DNA damage induced by simulate UV radiation exposure.

The evaluation of UV absorption properties of promising photoprotect agents is an essential feature for developing efficacious sunscreens products [31]. As a preliminary step of the present study, we performed the UV absorption screening profile of three benzofuroazepine compounds. All tested samples showed absorption spectrum in the UVA and UVB ranges, but the MBBA was the most promising molecule, possessing similar UV absorption spectrum to the selected standard UV filters. Considering its chemical structure, it is possible to suggest that the presence of methoxyl group, an electron-donating group, in association with the aromatic rings and unsaturated carbon bonds provided a superior UV light absorptive property in comparison with the other tested molecules. Polymeric nanoparticles have been widely investigated as UV filter carriers because of their biocompatibility with biological tissues as well as reduced cutaneous permeation of UV filters and the occurrence of phototoxicity events. In addition, due to their size and composition they can act as physical agents by scattering the UV rays, improving the photoprotection properties of a formulation by a positive effect to the UV filter entraped into oil core [31]. The next steps of the study focused in the developing of a nanostrucutured formulation by preparing nanocapsules.

The oil core is a structural component of the nanocapsules that may provide additional photoprotective properties to the formulation [32]. Concerning previous studies [32,33], the VIT E has been widely employed in sunscreens due to its antiaging, anti-inflammatory, and antioxidant properties. Besides, the VIT E protects against UV-induced DNA damage in skin, which highliths its potential application in the developing of sunscreen formulations [34]. In the scientific literature, there are no reports about the preparation of MBBA-loaded nanocapsule suspensions as well as the association of the Eudragit RS100® with the VIT E. As a

preformulation step, to ensure the formation and maintenance of this type of nanostructure, the chosen polymer must be insoluble in both oily and aqueous phases. Futhermore, the absence of polymer swelling by the oil is also required. In the present study, no significant modification in the weight of the polymeric films over time was observed, suggesting that the VIT E and the Eudragit RS100® polymer are compatible materials for developing a formulation of nanocapsules.

After preparing the nanostructures, a complete physicochemical characterization is required in order to elucidate the properties and stability profile of formulations. The interfacial deposition of preformed polymer method has been reported to incorporate high contents of lipophilic drugs into polymeric nanoparticles [35]. In this context, the MBBA-loaded nanocapsule suspensions presented appropriated parameters for a nanostructured formulation intended topical application, i.e., macroscopically homogeneous appearance, acid pH, unimodal particle distribution, and no significant loss of the total MBBA incorporated during the production of formulations. The laser diffraction technique showed absence of microparticles in nanocapsule suspensions, while the ZetaSizer® analysis revealed a mean particle size about 170 nm and low PDI. Collectively, these results confirm that the formulations had homogeneity of size distribution and particles in the nanometric range. The parameter of zeta potential values reflects the surface charge of nanoparticles, and as expected, the nanocapsule suspensions produced with Eudragit RS100® polymer exhinited positive values. This can explained through the cationic nature of polymer, which contains a quaternary ammonium group [36]. In addition, the pH values of he MBBA-loaded nanocapsule suspensions are compatible for cutaneous use, since the pH of the skin human is slightly acidic [17]. The MBBA-loaded nanocapsule suspensions showed a high encapsulation efficiency (EE=100%), which was expected due to the MBBA high lipophilic character, favoring the compound solubilization in the oil core. Our results are in agreement with previous studies [31,37], which demonstrated appropriate physicochemical characteristics of the nanocapsule suspensions containing standard UV filters. Another important feature about pharmaceutical products it the stability. After 60 days of storage no changes were observed in the macroscopic appearance, size, PDI, and pH. Despite this, an increase in zeta potential values were observed independent of the MBBA presence, which could be explained by chains relaxation of the Eudragit RS100® polymer, leading to quaternary ammonium group exposure [38].

An effective sunscreen should create a photostable protective film onto the outermost layer of the skin to absorb and/or reflect the UV radiation [39]. In this scenario, the use of some organic UV filters had some limitations due to their low photostability and phototoxicity.

Corroborating with this subject, Afonso and co-workes [13] showed that avobenzone (butyl methoxydibenzoylmethane), a standard UVA filter, loses the UV absorption property after exposure to the sunlight. In this study, the results obtained in the photostability evaluation demonstrated that the free or nanoencapsulated MBBA forms did not exhibit any content change caused by UV light, which reinforces the high stability of both compound and formulation. Therefore, these data suggest that the MBBA is promising as a photoprotect agent because it has a photostable profile and a broad-spectrum of absorption in the UVB and UVA ranges.

The results of i*n vitro* UV light absorptive/scatter potential suggested that MBBA-loaded nanocapsule suspensions simultaneously acts as a chemical and a physical UV filter. The results of UV spectrum of the $NC_{MBBA\text{-}MTC}$ showed broad spectrum of absorption at the UVB and UVA regions with maximum intensity at the UVB region. On the other hand, the UV spectrum of the $NC_{MBBA\text{-}VIT\ E}$ also showed maximum absorbance similarly to the $NC_{MBBA\text{-}MTC}$, but in a higher intensity. This can be explained by UV absorption property of VIT E [32] composing in the oil core of the $NC_{MBBA\text{-}VIT\ E}$. In addition, our results demonstrated that the light scattering produced by the blank nanocapsule sunspensions is not as effective as the absorption/scattering observed for the MBBA-loaded nanocapsule suspensions, reinforcing the critical role of MBBA in the photoprotective potential of the formulation.

The cationic polymeric nanoparticles have positive charges attached to their surface, which favour the interaction with the skin (negative charges) [40]. This bioadhesive property is a desired characteristic to sunscreen formulations because it may reduce the penetration on the skin [21]. In order to evaluate the bioadhesive potential of the MBBA-loaded nanocapsule suspensions, the interaction of nanoparticles and porcine mucin were assessed. The mucin human is the main component of mucus and have similar chemical and morphologic structures with porcine mucin, suggesting that porcine mucin may be a valuable model for estimating the bioadhesive potential of formulations [41]. Mucin molecules exhibit sialic acids linked to the terminal ends of the oligosaccharide chains, which provides negative charge to mucin [42]. The results of the present study showed that the MBBA-loaded nanocapsule suspensions, which had positive zeta potential, underwent an inversion of charge after the mucin exposure. This result suggested the high ability of the MBBA-loaded nanocapsule suspensions to interact with mucin by electrostatic attraction beetwen Eudragit RS100® polymer and mucin. Furthermore, a previous study suggested that the adsorption of mucin on the surface of nanoparticles could increase their size [43]. In fact, both formulations showed an increase of particle size suggesting particle agglomeration.

New substances and formulations require appropriate toxicological evaluation in preclinical steps before human use, especially those products intended to daily application [44]. In this sense, *in vitro* assays offer several advantages, such as fastness, reproductibility conditions, sensibility and reduced need of animal models [45]. Importantly, the HET-CAM test is an alternative screening assay to evaluate the potential irritation of formulations and their constituents [46]. In the present study, free or nanoencapsulated MBBA forms did not show irritant effect, which suggest that the developed formulations and raw materials used in their preparation caused no toxic consequences in the experimental conditions tested. In addition, as a complementary tool to the toxicological evaluation, the use of aquatic invertebrates has become prevalent, especially in the nanotoxicological field [47–49]. The *Artemia salina* is an invertebrate zooplankton found in various marine ecosystems and is used as an alternative experimental model for evaluate the toxicological potential [49]. In this study, the larvae of *A. salina* (instar I) was applied to estimate if the acute exposure to free MBBA or formulations would induce any toxic effect. Our results showed that after 24 h of incubation with free MBBA the % of survival was reduced in comparison with the control group, which was exposed to the vehicle. Importantly, MBBA nanoencapsulation abolish such toxic effect to *A. salina*, indicating an interesting advantage achieved by encapsulating the compound. Thus, the sets of toxicological tests perfomed in the current study highlight the low toxic potential of the formulations.

Considering the promising results showed by the developed of the MBBA-loaded nanocapsule suspensions, in a subsequent step the hydrogels containing nanocapsule suspensions were proposed because nanocapsule formulations were obtained as liquid form, hinder your topic application. Therefore, a gelling agent is necessary to achieve rheological and spreadability profiles suitable to cutaneous application. The gellan gum, a biocompatible and nontoxic microbial polysaccharide was applied as the dermatological base [50]. Our research group has been investigating in different studies the potential use of this gum to prepare nano-based hydrogels [23,24]. The results showed that the thickening process did not cause any negative impact on physicochemical characteristics of nanocapsules in comparison to those of the suspension (Size, PDI and pH values). Thus, these data indicated that the obtained hydrogels showed suitable properties intending cutaneous administration.

The photoprotective effectiveness of formulations may be estimated by inducting of erythema, a fast-physiologic skin response after the excessive exposure to sunlight. This inflammatory response can be easily visualized by the apparition of redness when exposure is above the minimal erythemal dose (MED). The ratio between the MED determined on the skin

bearing 2 mg cm^{-2} of sunscreen and on naked skin defines the sun protection factor (SPF) [8]. SPF value mostly reflects UVB photoprotection, because erythema is predominantly induced by this range of the solar spectrum. Thus, SPF value is not a complete sun protection factor because did not provide the potential photoprotect in the UVA range [51]. Nowdays, *in vitro* approaches based in transmission properties are used to estimate the photoprotection afforded by sunscreens in the UVA range (UVA-PF) [52].

An important issue regarding SPF as well as UVA-PF concerns their biological relevance in photoprotection. In fact, these parameters do not necessarily reflect other deleterious effects of UV radiation in biomolecules, such as DNA [29]. As far as genotoxicity, the evaluation of the prevention against DNA damage appears as a promissing additional parameter of photoprotection measure. Therefore, new methodologies to overcome such limitations of the current approaches for measuring photoprotection are necessary. In the present study, we applied an inovate strategy to evaluate the ability of hydrogels in protecting DNA against the photodamage induced by UVB and UVA radiation. All hydrogels effectively prevented the DNA photoproducts formation when compared with the unprotected irradiated DNA samples (vehicle), demonstrating high potential of DNA protection against simulated UVB and UVA exposure.

In conclusion, the current study showed the identification of a compound with promising UV absorptive potential and the preparation of a final nano-based hydrogel formulation for cutaneous application. The results demonstrated that the nanocapsules were successfully developed, possessing suitable nanometric size, mucoadhesive property and high photostability profile. In addition, the hydrogels containing MBBA-loaded nanocapsules had adequate physicochemical properties and were with effective in protecting the DNA against UV radiation damage.

5. Funding Information/Acknowledgements

We gratefully acknowledge Universidade Federal de Santa Maria (UFSM), Fundação de Amparo a Pesquisa do Estado do Rio Grande do Sul (FAPERGS, grant number 17/2551-0000), Conselho Nacional de Desenvolvimento Científico e Tecnológico (CNPq, grant number 407118/2018-7), and Coordenação de Aperfeiçoamento de Pessoal de Nível Superior (CAPES/PROEX #23038.004173/2019-93) for the financial support. C.W.N is recipient of CNPq fellowship (#304864/2015-3).

6. Conflict of interest

The authors declare that they have no conflict of interest.

7. References

[1] V.T. Natarajan, P. Ganju, A. Ramkumar, R. Grover, R.S. Gokhale, Multifaceted pathways protect human skin from UV radiation, Nat. Chem. Biol. 10 (2014) 542–551. doi:10.1038/nchembio.1548.

[2] S. Roy, Impact of UV Radiation on Genome Stability and Human Health, (2017) 207–219. doi:10.1007/978-3-319-56017-5_17.

[3] C.P. dos Santos, J.E.L. Londero, M.B. dos Santos, R. dos S. Feltrin, L. Loebens, L.B. Moura, S.Z. Cechin, A.P. Schuch, Sunlight-induced genotoxicity and damage in keratin structures decrease tadpole performance, J. Photochem. Photobiol. B Biol. 181 (2018) 134–142. doi:10.1016/j.jphotobiol.2018.03.013.

[4] B. Cortat, C.C.M. Garcia, A. Quinet, A.P. Schuch, K.M. De Lima-Bessa, C.F.M. Menck, The relative roles of DNA damage induced by UVA irradiation in human cells, Photochem. Photobiol. Sci. 12 (2013) 1483–1495. doi:10.1039/c3pp50023c.

[5] A.P. Schuch, C.C.M. Garcia, K. Makita, C.F.M. Menck, DNA damage as a biological sensor for environmental sunlight, Photochem. Photobiol. Sci. 12 (2013) 1259–1272. doi:10.1039/c3pp00004d.

[6] A.P. Schuch, N.C. Moreno, N.J. Schuch, C.F.M. Menck, C.C.M. Garcia, Sunlight damage to cellular DNA: Focus on oxidatively generated lesions, Free Radic. Biol. Med. 107 (2017) 110–124. doi:10.1016/j.electacta.2018.01.181.

[7] S. Singer, S. Karrer, M. Berneburg, Modern sun protection, Curr. Opin. Pharmacol. 46 (2019) 24–28. doi:10.1016/j.coph.2018.12.006.

[8] M. Krause, A. Klit, M. Blomberg Jensen, T. Søeborg, H. Frederiksen, M. Schlumpf, W. Lichtensteiger, N.E. Skakkebaek, K.T. Drzewiecki, Sunscreens: Are they beneficial for health? An overview of endocrine disrupting properties of UV-filters, Int. J. Androl. 35 (2012) 424–436. doi:10.1111/j.1365-2605.2012.01280.x.

[9] M.S. Latha, J. Martis, V. Shobha, R.S. Shinde, S. Bangera, B. Krishnankutty, S. Bellary, S. Varughese, P. Rao, B.R.N. Kumar, Sunscreening agents: A review, J. Clin. Aesthet. Dermatol. 6 (2013) 16–26.

[10] A.R. Young, J. Claveau, A.B. Rossi, Ultraviolet radiation and the skin: Photobiology and

sunscreen photoprotection, J. Am. Acad. Dermatol. 76 (2017) S100–S109. doi:10.1016/j.jaad.2016.09.038.

[11] C. Berkey, N. Oguchi, K. Miyazawa, R. Dauskardt, Role of sunscreen formulation and photostability to protect the biomechanical barrier function of skin, Biochem. Biophys. Reports. 19 (2019) 100657. doi:10.1016/j.bbrep.2019.100657.

[12] M.E. Burnett, S.Q. Wang, Current sunscreen controversies: A critical review, Photodermatol. Photoimmunol. Photomed. 27 (2011) 58–67. doi:10.1111/j.1600-0781.2011.00557.x.

[13] S. Afonso, K. Horita, J.P. Sousa E Silva, I.F. Almeida, M.H. Amaral, P.A. Lobão, P.C. Costa, M.S. Miranda, J.C.G. Esteves Da Silva, J.M. Sousa Lobo, Photodegradation of avobenzone: Stabilization effect of antioxidants, J. Photochem. Photobiol. B Biol. 140 (2014) 36–40. doi:10.1016/j.jphotobiol.2014.07.004.

[14] J.B. Mancuso, R. Maruthi, S.Q. Wang, H.W. Lim, Sunscreens: An Update, Am. J. Clin. Dermatol. 18 (2017) 643–650. doi:10.1007/s40257-017-0290-0.

[15] S. Montalvo-Quiros, J.L. Luque-Garcia, Combination of bioanalytical approaches and quantitative proteomics for the elucidation of the toxicity mechanisms associated to TiO 2 nanoparticles exposure in human keratinocytes, Food Chem. Toxicol. 127 (2019) 197–205. doi:10.1016/j.fct.2019.03.036.

[16] R. Gai, D.F. Back, G. Zeni, Potassium tert-Butoxide-Catalyzed Synthesis of Benzofuroazepines via Cyclization of (2-Alkynylbenzyl)oxy Nitriles, J. Org. Chem. 80 (2015) 10278–10287. doi:10.1021/acs.joc.5b01884.

[17] D. Papakostas, F. Rancan, W. Sterry, U. Blume-Peytavi, A. Vogt, Nanoparticles in dermatology, Arch. Dermatol. Res. 303 (2011) 533–550. doi:10.1007/s00403-011-1163-7.

[18] K. Paese, A. Jäger, F.S. Poletto, E.F. Pinto, B. Rossi-Bergmann, A.R. Pohlmann, S.S. Guterres, Semisolid formulation containing a nanoencapsulated sunscreen: Effectiveness, in vitro photostability and immune response, J. Biomed. Nanotechnol. 5 (2009) 240–246. doi:10.1166/jbn.2009.1028.

[19] K. Coradini, K. Paese, R.C. Beck, F.N. Fonseca, S.S. Guterres, C.B. Detoni, A.R. Pohlmann, Poly(ϵ-caprolactone) microcapsules and nanocapsules in drug delivery, Expert Opin. Drug Deliv. 10 (2013) 623–638. doi:10.1517/17425247.2013.769956.

[20] S.A. Wissing, R.H. Müller, The development of an improved carrier system for sunscreen formulations based on crystalline lipid nanoparticles, Int. J. Pharm. 242 (2002) 373–375. doi:10.1016/S0378-5173(02)00219-3.

[21] M.E. Parente, A. Ochoa Andrade, G. Ares, F. Russo, A. Jiménez-Kairuz, Bioadhesive hydrogels for cosmetic applications, Int. J. Cosmet. Sci. 37 (2015) 511–518. doi:10.1111/ics.12227.

[22] L.A. Frank, P.D.S. Chaves, A.R. Pohlmann, A.G. Frank, R.C.R. Beck, S.S. Guterres, Mucoadhesive Properties of Eudragit®RS100, Eudragit®S100, and Poly(ε-caprolactone) Nanocapsules: Influence of the Vehicle and the Mucosal Surface, AAPS PharmSciTech. 19 (2018) 1637–1646. doi:10.1208/s12249-018-0968-5.

[23] M.C.L. Marchiori, C. Rigon, C. Camponogara, S.M. Oliveira, L. Cruz, Hydrogel containing silibinin-loaded pomegranate oil based nanocapsules exhibits anti-inflammatory effects on skin damage UVB radiation-induced in mice, J. Photochem. Photobiol. B Biol. 170 (2017) 25–32. doi:10.1016/j.jphotobiol.2017.03.015.

[24] N.S. Pegoraro, A. V. Barbieri, C. Camponogara, J. Mattiazzi, E.S. Brum, M.C.L. Marchiori, S.M. Oliveira, L. Cruz, Nanoencapsulation of coenzyme Q10 and vitamin E acetate protects against UVB radiation-induced skin injury in mice, Colloids Surfaces B Biointerfaces. 150 (2017) 32–40. doi:10.1016/j.colsurfb.2016.11.013.

[25] H. Takeuchi, J. Thongborisute, Y. Matsui, H. Sugihara, H. Yamamoto, Y. Kawashima, Novel mucoadhesion tests for polymers and polymer-coated particles to design optimal mucoadhesive drug delivery systems, Adv. Drug Deliv. Rev. 57 (2005) 1583–1594. doi:10.1016/j.addr.2005.07.008.

[26] N.P. LÜPKE, The hen’s egg test (HET)—an alternative toxicity test, Br. J. Dermatol. 115 (1986) 133–135. doi:10.1111/j.1365-2133.1986.tb02123.x.

[27] P. Vanhaecke, G. Persoone, Report on an Intercalibration Exercise on a Short-term Standard Toxicity Test with Artemia Nauplii (Arc-Test), Inserm. 106 (1981) 359–376.

[28] L.A. Rigo, W. Julia, C.B. Silva, R.C.R. Beck, Evaluation of the spreadability of pharmaceutical or cosmetic semisolid formulations using scanned images, Lat. Am. J. Pharm. 31 (2012) 1387–1391.

[29] M. Ben Said, M. Otaki, Development of a DNA-dosimeter system for monitoring the effects of pulsed ultraviolet radiation, Ann. Microbiol. 63 (2013) 1057–1063. doi:10.1007/s13213-012-0562-0.

[30] D.T. Ribeiro, C. Madzak, A. Sarasin, P. DI Mascio, H. Sies, C.F.M. Menck, Singlet Oxygen Induced Dna Damage and Mutagenicity in a Single-Stranded Sv40-Based Shuttle Vector, Photochem. Photobiol. 55 (1992) 39–45. doi:10.1111/j.1751-1097.1992.tb04207.x.

[31] E. Gilbert, L. Roussel, C. Serre, R. Sandouk, D. Salmon, P. Kirilov, M. Haftek, F. Falson,

F. Pirot, Percutaneous absorption of benzophenone-3 loaded lipid nanoparticles and polymeric nanocapsules: A comparative study, Int. J. Pharm. 504 (2016) 48–58. doi:10.1016/j.ijpharm.2016.03.018.

[32] S. Gause, A. Chauhan, UV-blocking potential of oils and juices, Int. J. Cosmet. Sci. 38 (2016) 354–363. doi:10.1111/ics.12296.

[33] B. Brownlow, V.J. Nagaraj, A. Nayel, M. Joshi, T. Elbayoumi, Development and in Vitro Evaluation of Vitamin E-Enriched Nanoemulsion Vehicles Loaded with Genistein for Chemoprevention Against UVB-Induced Skin Damage, J. Pharm. Sci. 104 (2015) 3510–3523. doi:10.1002/jps.24547.

[34] G.J. Delinasios, M. Karbaschi, M.S. Cooke, A.R. Young, Vitamin E inhibits the UVAI induction of “light” and “dark” cyclobutane pyrimidine dimers, and oxidatively generated DNA damage, in keratinocytes, Sci. Rep. 8 (2018) 1–12. doi:10.1007/s11664-013-2807-5.

[35] M.H. Marcondes Sari, L.M. Ferreira, V.A. Zborowski, P.C.O. Araujo, V.F. Cervi, C.A. Brüning, L. Cruz, C.W. Nogueira, p,p′-Methoxyl-diphenyl diselenide-loaded polymeric nanocapsules are chemically stable and do not induce toxicity in mice, 2017. doi:10.1016/j.ejpb.2017.03.018.

[36] R. Pignatello, C. Bucolo, P. Ferrara, A. Maltese, A. Puleo, G. Puglisi, Eudragit RS100® nanosuspensions for the ophthalmic controlled delivery of ibuprofen, Eur. J. Pharm. Sci. 16 (2002) 53–61. doi:10.1016/S0928-0987(02)00057-X.

[37] N.M. Siqueira, R. V. Contri, K. Paese, R.C.R. Beck, A.R. Pohlmann, S.S. Guterres, Innovative sunscreen formulation based on benzophenone-3-loaded chitosan-coated polymeric nanocapsules, Skin Pharmacol. Physiol. 24 (2011) 166–174. doi:10.1159/000323273.

[38] R. V. Contri, L.A. Fiel, N. Alnasif, A.R. Pohlmann, S.S. Guterres, M. Schäfer-Korting, Skin penetration and dermal tolerability of acrylic nanocapsules: Influence of the surface charge and a chitosan gel used as vehicle, Int. J. Pharm. 507 (2016) 12–20. doi:10.1016/j.ijpharm.2016.03.046.

[39] A.C. Cozzi, P. Perugini, S. Gourion-Arsiquaud, Comparative behavior between sunscreens based on free or encapsulated UV filters in term of skin penetration, retention and photo-stability, Eur. J. Pharm. Sci. 121 (2018) 309–318. doi:10.1016/j.ejps.2018.06.001.

[40] B. Balzus, F.F. Sahle, S. Hönzke, C. Gerecke, F. Schumacher, S. Hedtrich, B. Kleuser, R. Bodmeier, Formulation and ex vivo evaluation of polymeric nanoparticles for

controlled delivery of corticosteroids to the skin and the corneal epithelium, Eur. J. Pharm. Biopharm. 115 (2017) 122–130. doi:10.1016/j.ejpb.2017.02.001.

[41] B.J. Teubl, M. Absenger, E. Fröhlich, G. Leitinger, A. Zimmer, E. Roblegg, The oral cavity as a biological barrier system: Design of an advanced buccal in vitro permeability model, Eur. J. Pharm. Biopharm. 84 (2013) 386–393. doi:10.1016/j.ejpb.2012.10.021.

[42] R. Bansil, B.S. Turner, Mucin structure, aggregation, physiological functions and biomedical applications, Curr. Opin. Colloid Interface Sci. 11 (2006) 164–170. doi:10.1016/j.cocis.2005.11.001.

[43] P. dos S. Chaves, A.F. Ourique, L.A. Frank, A.R. Pohlmann, S.S. Guterres, R.C.R. Beck, Carvedilol-loaded nanocapsules: Mucoadhesive properties and permeability across the sublingual mucosa, Eur. J. Pharm. Biopharm. 114 (2017) 88–95. doi:10.1016/j.ejpb.2017.01.007.

[44] S. Inomata, Safety Assurance of Cosmetic in Japan: Current Situation and Future Prospects, J. Oleo Sci. 63 (2013) 1–6. doi:10.5650/jos.ess13501.

[45] S.K. Doke, S.C. Dhawale, Alternatives to animal testing: A review, Saudi Pharm. J. 23 (2015) 223–229. doi:10.1016/j.jsps.2013.11.002.

[46] D.C. Vinhal, R. Menegatti, L.C. Moreira, L. de Brito Rodrigues, G.A.R. de Oliveira, M.C. Valadares, Toxicity evaluation of the photoprotective compound LQFM048: Eye irritation, skin toxicity and genotoxic endpoints, Toxicology. 376 (2017) 83–93. doi:10.1016/j.tox.2016.04.007.

[47] S. Rajabi, A. Ramazani, M. Hamidi, T. Naji, Artemia salina as a model organism in toxicity assessment of nanoparticles, DARU, J. Pharm. Sci. 23 (2015) 1–6. doi:10.1186/s40199-015-0105-x.

[48] M. Bhuvaneshwari, V. Thiagarajan, P. Nemade, N. Chandrasekaran, A. Mukherjee, Toxicity and trophic transfer of P25 TiO2 NPs from Dunaliella salina to Artemia salina: Effect of dietary and waterborne exposure, Environ. Res. 160 (2018) 39–46. doi:10.1016/j.envres.2017.09.022.

[49] S. Zhu, F. Luo, W. Chen, B. Zhu, G. Wang, Toxicity evaluation of graphene oxide on cysts and three larval stages of Artemia salina, Sci. Total Environ. 595 (2017) 101–109. doi:10.1016/j.scitotenv.2017.03.224.

[50] M.M. Fiume, B. Heldreth, W.F. Bergfeld, D. V. Belsito, R.A. Hill, C.D. Klaassen, D.C. Liebler, J.G. Marks, R.C. Shank, T.J. Slaga, P.W. Snyder, F.A. Andersen, L.J. Gill, Safety Assessment of Microbial Polysaccharide Gums as Used in Cosmetics, Int. J. Toxicol. 35 (2016) 5S–49S. doi:10.1177/1091581816651606.

[51] S. Mouret, P. Bogdanowicz, M.J. Haure, N. Castex-Rizzi, J. Cadet, A. Favier, T. Douki, Assessment of the photoprotection properties of sunscreens by chromatographic measurement of DNA damage in skin explants, Photochem. Photobiol. 87 (2011) 109–116. doi:10.1111/j.1751-1097.2010.00834.x.

[52] C. Stiefel, W. Schwack, Photoprotection in changing times - UV filter efficacy and safety, sensitization processes and regulatory aspects, Int. J. Cosmet. Sci. 37 (2015) 2–30. doi:10.1111/ics.12165.

FIGURE CAPTIONS

Figure 1: UV light absorptive spectrum and the chemical structures of the 6-(4-methoxyphenyl)-5H-benzo[d]benzofuro[3,2-b]azepine (MBBA – green line), (*p*-aminobenzoic acid (PABA – reed line) and benzophenone 3 (BZ3 – purple line) at concentration of 10µg/mL.

Figure 2: *In vitro* UV light absorptive/scatter spectrum of the MBBA-loaded nanocapsules; $NC_{MBBA\text{-}VIT\ E}$ **(2A** – orange line**)** and $NC_{MBBA\text{-}MTC}$ **(2B** – blue line**)** at concentration of 10µg/mL.

Figure 3: Mean particle size **(3A)** and zeta potential **(3B)** before (basal measures) and after mucin contact (Mucin 0.1%). The values are reported as mean ± S.E.M; n=3/formulation; * denotes the significant difference when compared to the respective basal measure ($p<0.05$; Two-way ANOVA followed by the Tukey's test).

Figure 4: Representative images of the chorioallantoic membrane (CAM) after the application of $NC_{MBBA\text{-}MTC}$ **(A)**, $NC_{B\text{-}MCT}$ **(B)**, $NC_{MBBA\text{-}VIT\ E}$ **(C)**, $NC_{B\text{-}VIT\ E}$ **(D)**, MBBA free **(E)**, 0.1N NaOH - positive control **(F)**, 1% SLS - positive control **(G)** and salina solution - negative control **(H)**.

Figure 5: DNA lesions after exposure to the simulated UVB and UVA light. Representative image of the electrophoresis in the presence of the DNA repair enzymes, T4-endo V or Fpg **(5A)**. The quantity of DNA lesions induced by UVB **(5B)** or UVA **(5C)** in the absence or presence of the hydrogels. Abbreviations: FI (supercoiled plasmid DNA bands); FII (open-circular relaxed DNA bands); T4 (T4-endo V sensitive sites – CPDs); Fpg (Fpg sensitive sites – oxidised DNA bases). The values are reported as mean ± S.E.M of the 3 independent experiments.

FIGURES

Figure 1:

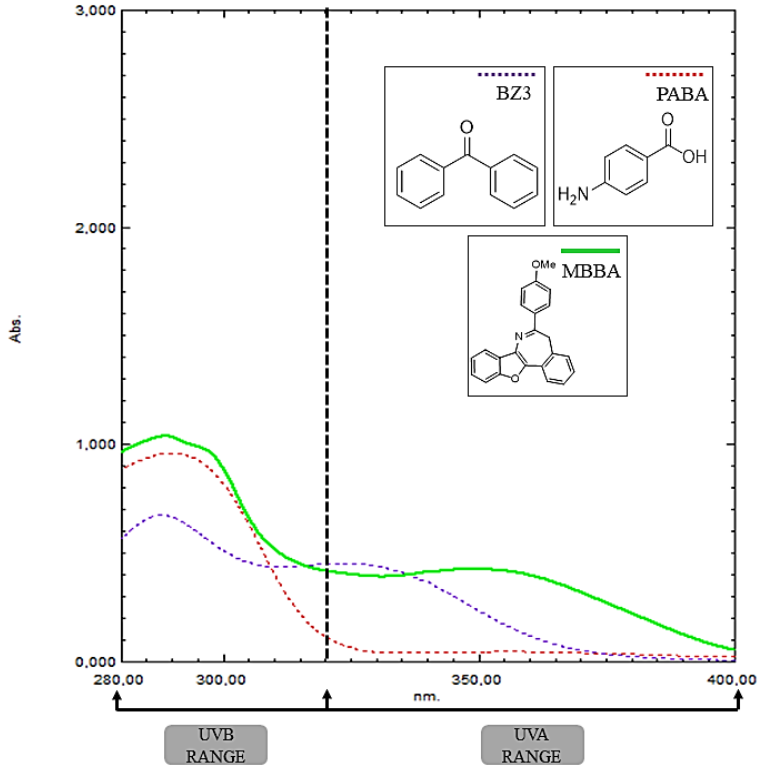

Figure 2A:

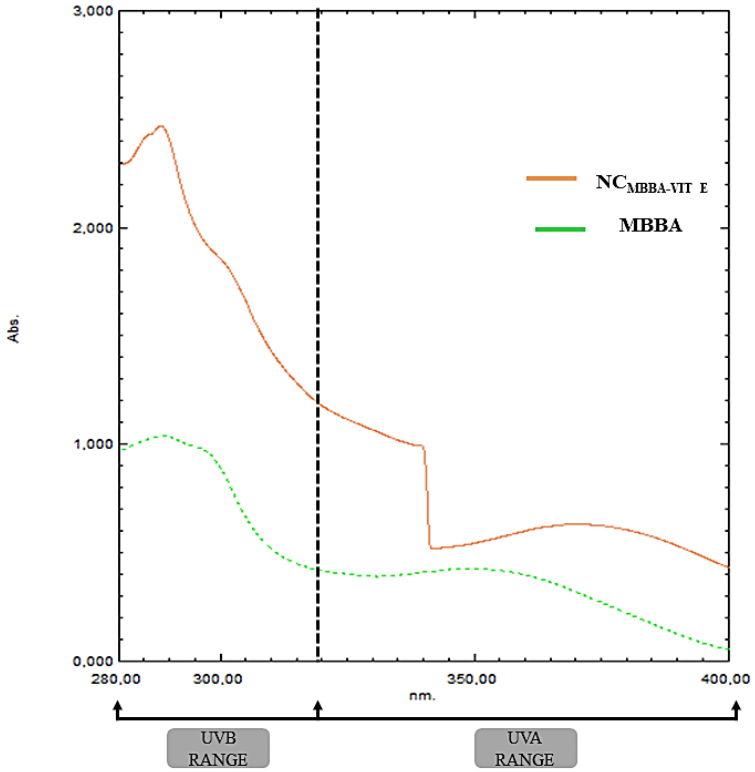

Figure 2B:

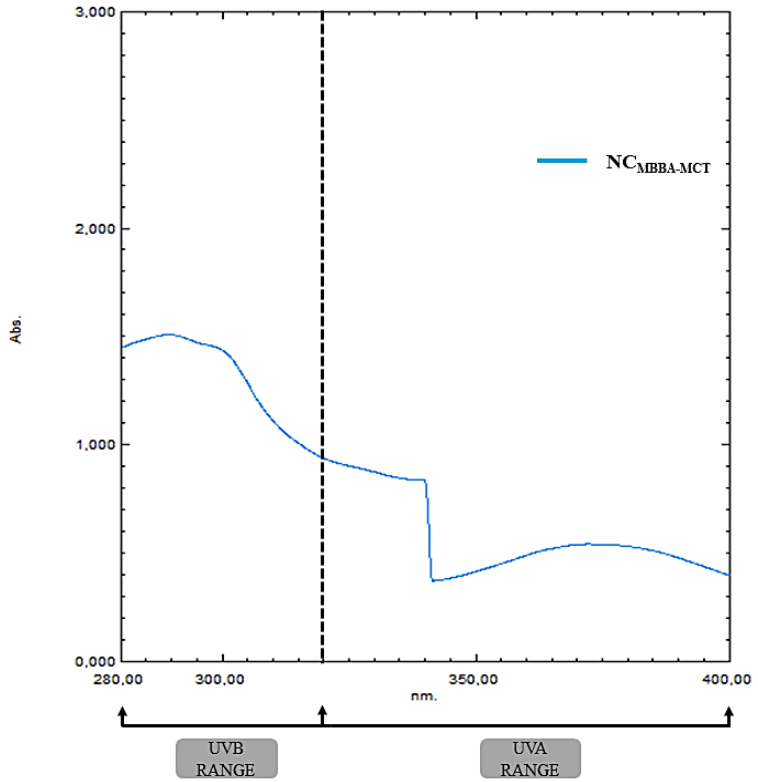

Figure 3A:

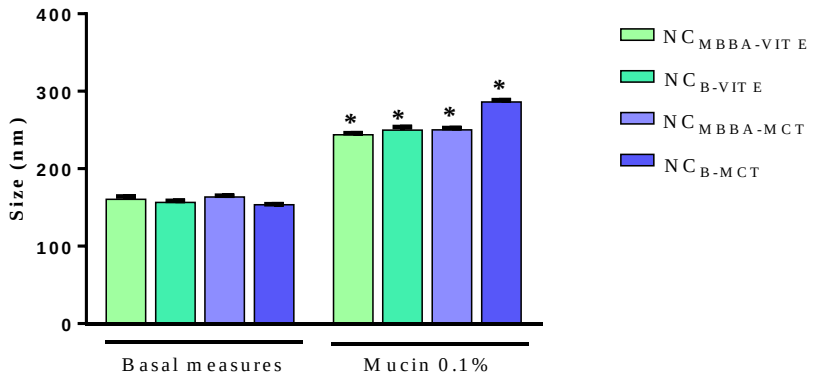

Figure 3B:

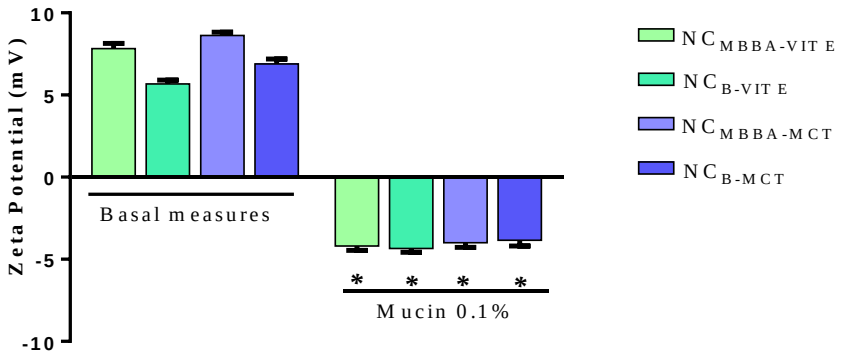

Figure 4:

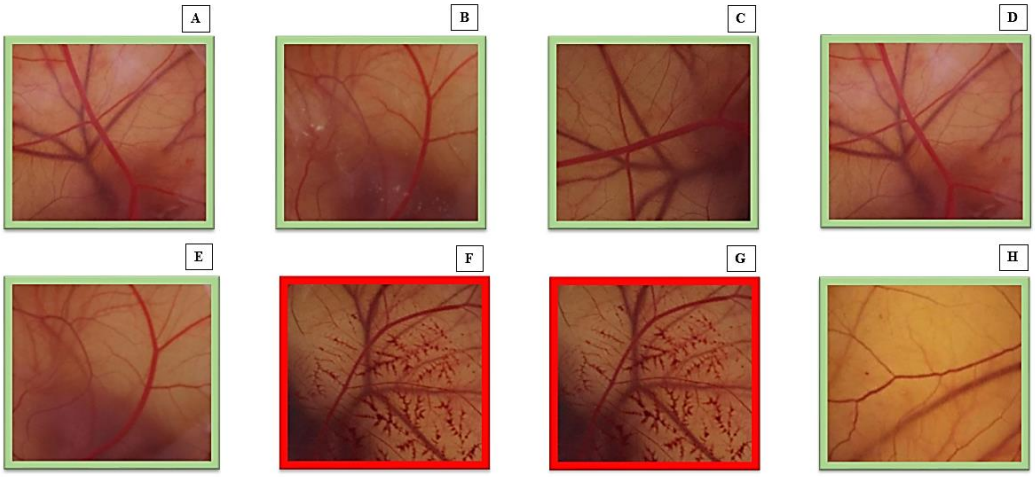

Figure 5A:

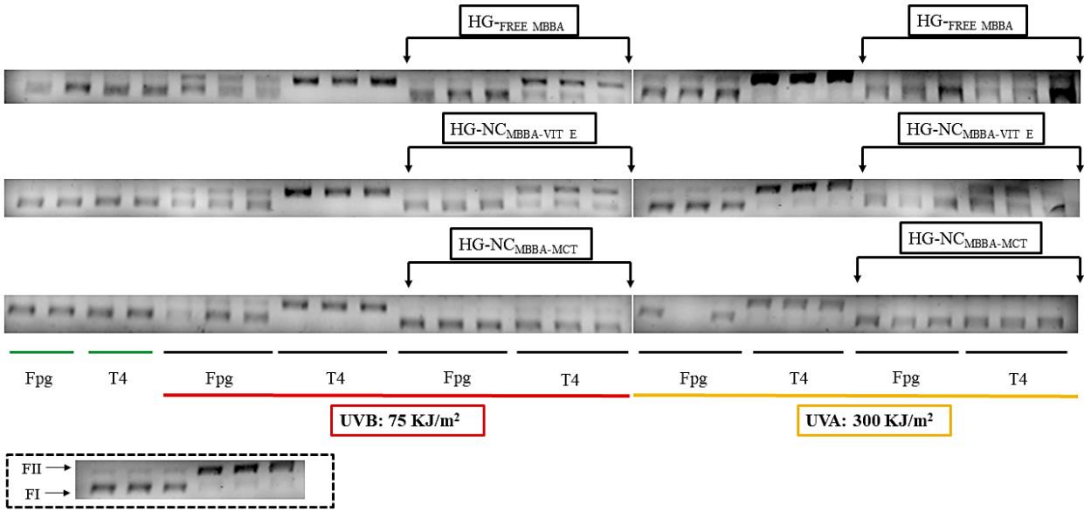

Figure 5B:

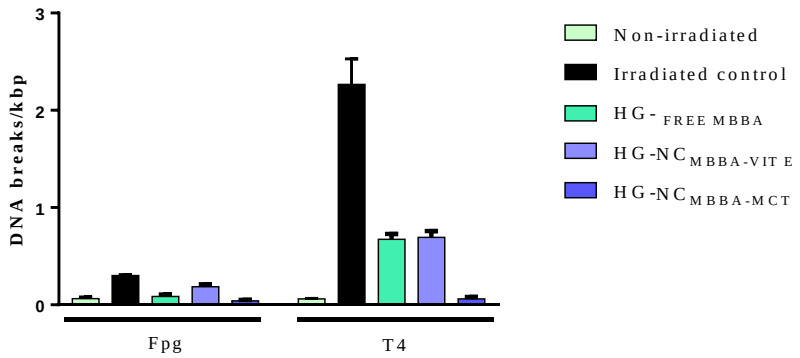

Figure 5C:

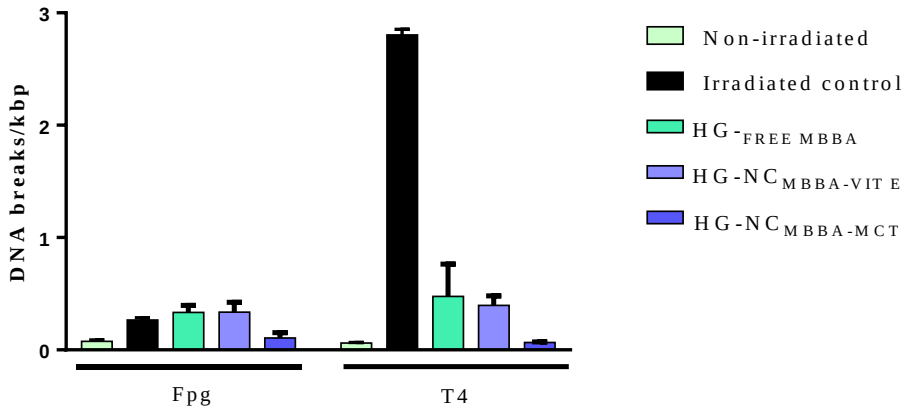
DNA breaks/kbp
3
2
1
0
Fpg
T4
Non-irradiated
Irradiated control
HG-FREE MBBA
HG-NCMBBA-VIT E
HG-NCMBBA-MCT

TABLES

Tabela 1: The qualitative and quantitative composition of each developed formulation.

	Formulation composition			
Organic phase	$NC_{MBBA\text{-}VIT\ E}$	$NC_{B\text{-}VIT\ E}$	$NC_{MBBA\text{-}MCT}$	$NC_{B\text{-}MCT}$
Eudragit RS100® (g)	0.100	0.100	0.100	0.100
Span® 80 (g)	0.077	0.077	0.077	0.077
VIT E oil (µL)	330	330	-	-
MCT oil (µL)	-	-	330	330
Acetone (mL)	54	54	54	54
MBBA (g)	0.015	0.015	-	-
Aqueous phase				
Tween® 80 (g)	0.077	0.077	0.077	0.077
Water (mL)	54	54	54	54

Span® 80: Sorbitan monooleate; VIT E: vitamin E acetate; MCT: medium chain triglycerides; Tween® 80: polysorbate 80

Tabela 2: Physicochemical characteristics of the MBBA-loaded nanocapsule suspensions (NCMBBA-VIT E and NCMBBA-MCT) and their respective unloaded (blank) formulations (NCB -VIT E and NCB-MCT) at initial time.

	Parameters				
Formulations	Size (nm)	PDI[a]	ZP[b] (mV)	pH	MBBA content (%)
$NC_{MBBA\text{-}VIT\ E}$	153±1	0.12±0.00	9.2±0.8	5.2±0.1	99.6±0.7
$NC_{B\ \text{-}VIT\ E}$	174±1	0.07±0.00	7.1±0.3	5.0±0.0	-
$NC_{MBBA\text{-}MCT}$	162±9	0.12±0.02	8.4±0.5	5.0±0.0	100.5±0.9
$NC_{B\text{-}MCT}$	168±2	0.09±0.01	7.3±0.5	5.2±0.0	-

The values are reported as mean ± S.E.M of 3/formulation. The data were analyzed using a One-way of variance (ANOVA) $p>0.05$.

[a]PDI: Polydispersity Index

[b]ZP: Zeta Potential

Tabela 3: Laser diffraction analyses of the MBBA-loaded nanocapsules suspensions (NCMBBA-VIT E and NCMBBA-MCT) and their respective unloaded (blank) formulations (NCB -VIT E and NCB-MCT) at initial time.

	Parameters	
	D[4:3]	SPAN
$NC_{MBBA\text{-}VIT\ E}$	0.267±0.008	0.834±0.030
$NC_{B\ \text{-}VIT\ E}$	0.284±0.014	0.892±0.094
$NC_{MBBA\text{-}MCT}$	0.348±0.011	1.382±0.115
$NC_{B\text{-}MCT}$	0.376±0.034	1.316±0.174

The values are reported as mean ± S.E.M of 3/formulation. The data were analyzed using a One-way of variance (ANOVA) $p>0.05$.

Tabela 4: Effects of MBBA-loaded nanocapsule suspensions on the Artemia salina lethality.

	Survival rate (%)					
Groups	2.5 µg/mL	5 µg/mL	10 µg/mL	15 µg/mL	25 µg/mL	50 µg/mL
FREE MBBA	100	100	100	70	50	0
$NC_{MBBA\text{-}VIT\ E}$	100	100	100	100	100	100
$NC_{B\text{-}VIT\ E}$	100	100	100	100	100	100
$NC_{MBBA\text{-}MCT}$	100	100	100	100	100	100
$NC_{B\text{-}MCT}$	100	100	100	100	100	100
VEHICLE (WATER)	100	100	100	100	100	100
VEHICLE (DMSO)	100	100	100	100	100	100

The values are reported as mean of three independent experiments (n=3/group).

Tabela 5: Physicochemical characterization of hydrogels.

	Parameters				
Formulations	Size (nm)	PDI[a]	pH	MBBA content (%)	Sf[b] (mm^2/g)
HG-$NC_{MBBA\text{-}VIT\ E}$	222±5	0.21±0.02	5.7±0.0	97.6±0.7	3.2
HG-$NC_{B\text{-}VIT\ E}$	197±3	0.14±0.02	5.8±0.0	-	3.3
HG-$NC_{MBBA\text{-}MCT}$	196±3	0.21±0.03	5.7±0.1	96.5±0.9	2.9
HG-$NC_{B\text{-}MCT}$	194±6	0.15±0.01	5.5±0.0	-	2.8
HG- $_{FREE\text{-}MBBA}$	-	-	5.5±0.0	97.3±0.6	2.7
HG- $_{VEICHLHE}$	-	-	5.9±0.0	-	2.9

The values are reported as mean ± S.E.M of 3/formulation. The data were analyzed using the One-way of variance (ANOVA) $p>0.05$.

[a]PDI: Polydispersity Index

[b]Sf: Spreadability factor

Tabela 6: DNA photoprotection properties provided by hydrogels.

	Parameters			
	% Protection UVB	SPF-DNA[a] UVB	% Protection UVA	SPF-DNA UVA
Formulations				
HG-$_{FREE-MBBA}$	73.5±2.1	3.8±0.3	72.5±11.5	4.3±2.2
HG-NC$_{MBBA-VIT\ E}$	69.5±3.7	3.3±0.4	75.2±9.6	4.4±1.6
HG-NC$_{MBBA-MCT}$	96.9±0.5	33.4±5.3	95.3±0.1	21.2±0.6

The values are reported as mean ± S.E.M of the 3 independent experiments

[a]SPF-DNA: Sun Protection Factor for the DNA;

SUPPLEMENTARY MATERIAL

Development of a nontoxic nanotechnological-based hydrogel containing a novel benzofuroazepine compound with potential photoprotective properties

Vinicius Costa Prado[1]; Marcel Henrique Marcondes Sari[2]; Bruna Cogo Borin[3]; Roberto do Carmo[1]; Letícia Cruz[2]; André Schuch[3]; Cristina Wayne Nogueira[1]; Gilson Zeni*[1]

Figure 1AS:

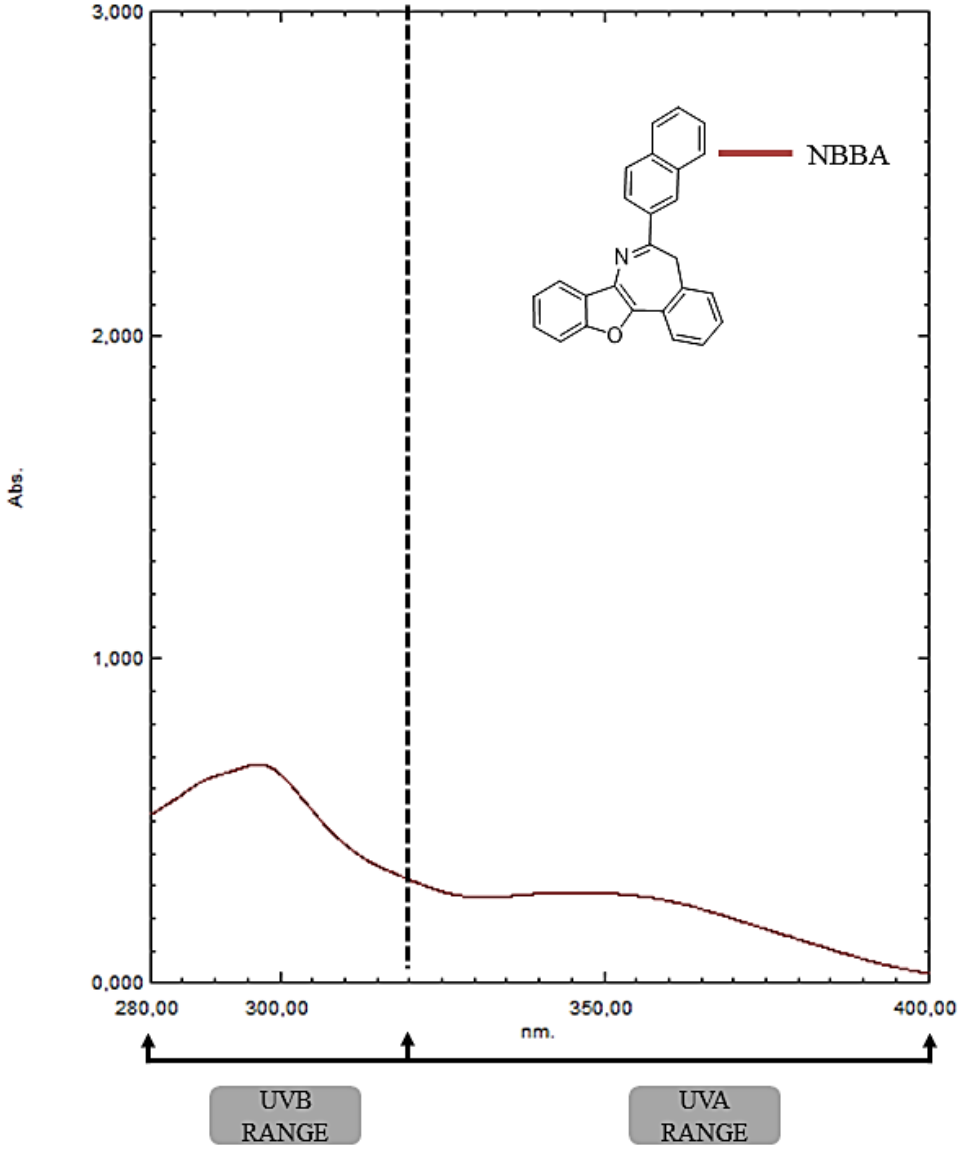

Figure 1BS:

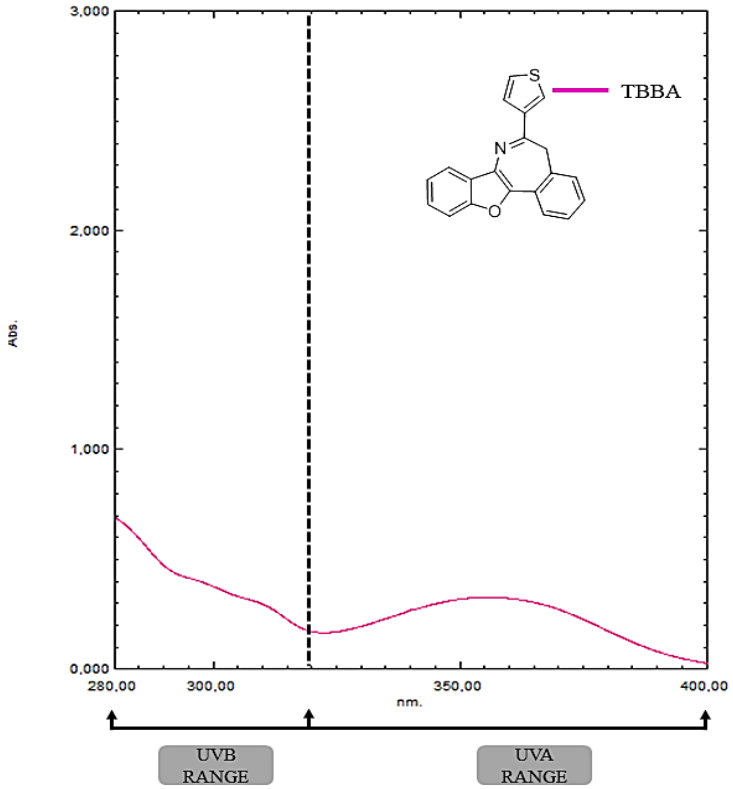

Figure 1CS:

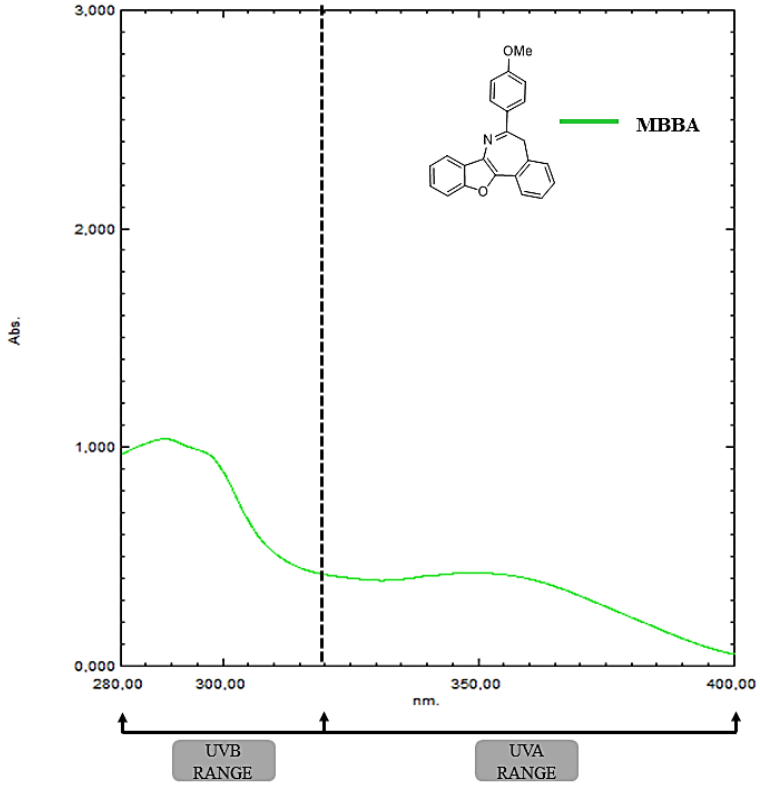

Figure 1S: UV light absorptive representative spectrum and chemical structures of benzofuroazepine compounds, 6(naphthalen)-5H-benzo[d]benzofuro[3,2-b]azepine (NBBA) **(1AS)**; 6-(thiophen-3-yl)-5H-benzo[d]benzofuro[3,2-b]azepine (TBBA) **(1BS)**, and 6-(4-methoxyphenyl)-5H-benzo[d]benzofuro[3,2-b]azepine (MBBA) **(1CS)**.

Figure 2AS:

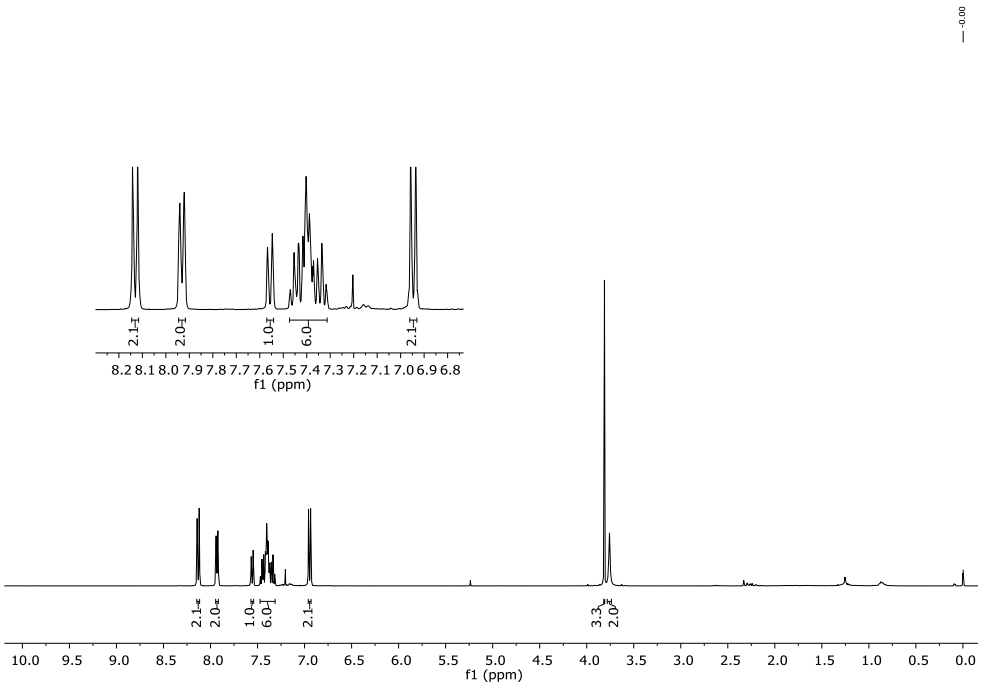

Figure 2BS:

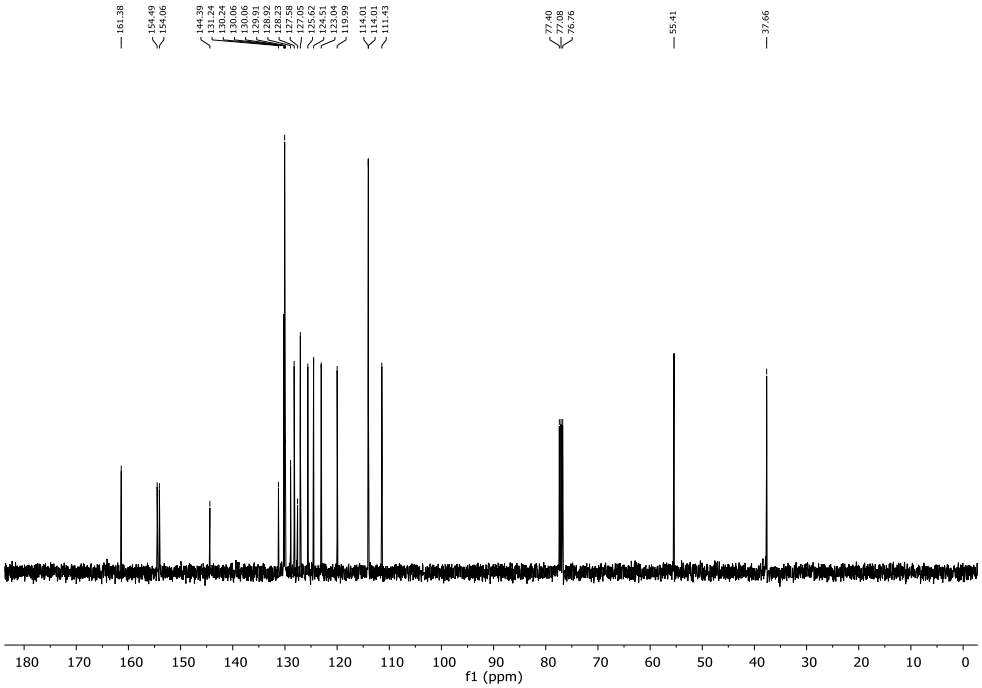

Figure 2S: The ^{1}H (400 MHz) NMR (2AS) and the ^{13}C (100 MHz) NMR spectra (2BS) of MBBA compound in chloroform ($CDCl_3$).

Figure 3AS:

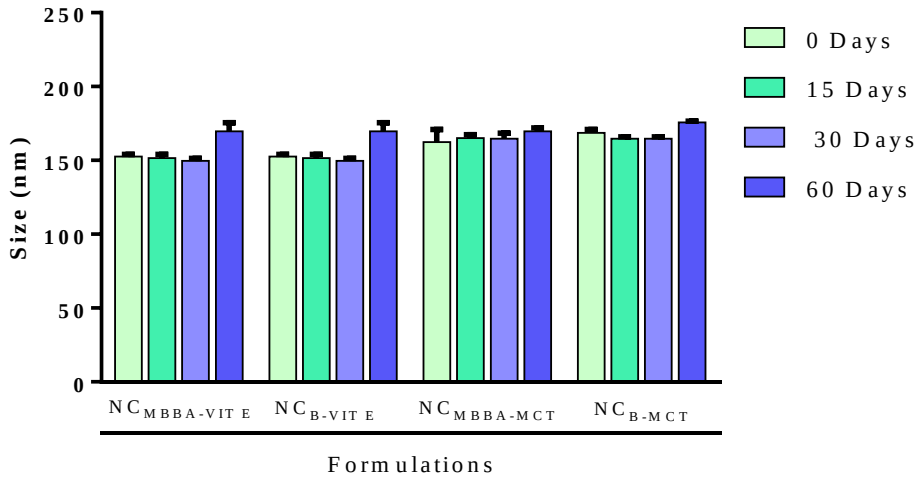

Figure 3BS:

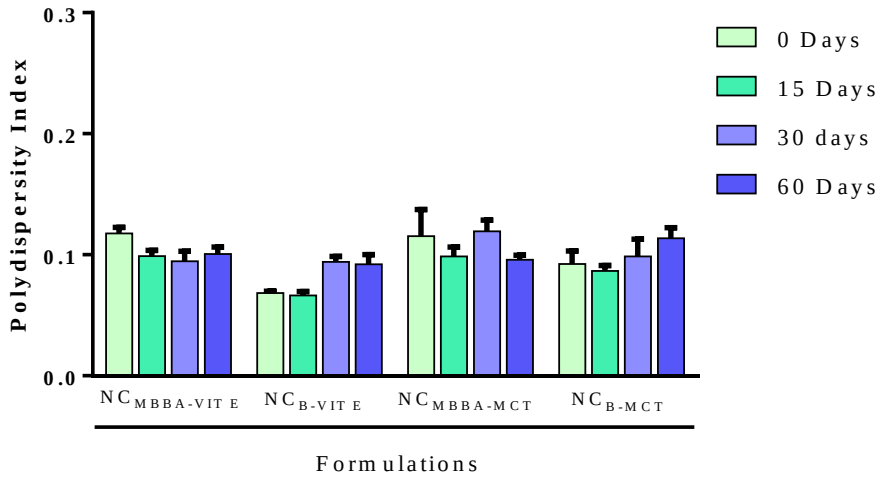

Figure 3CS:

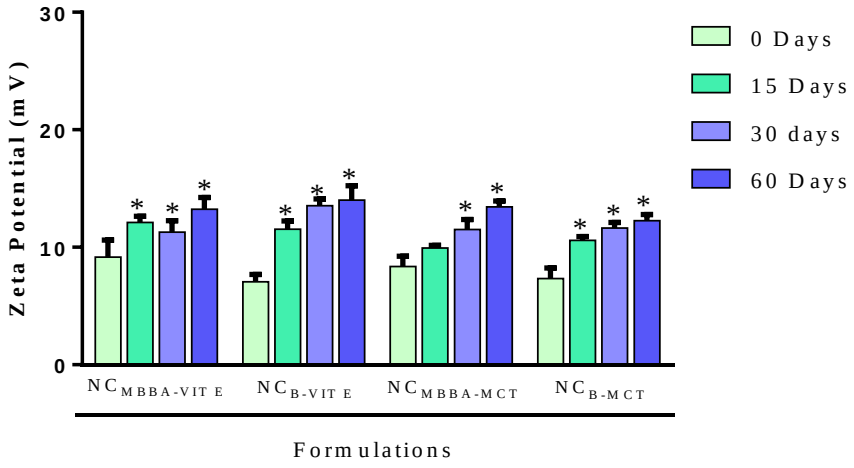

Figure 3DS:

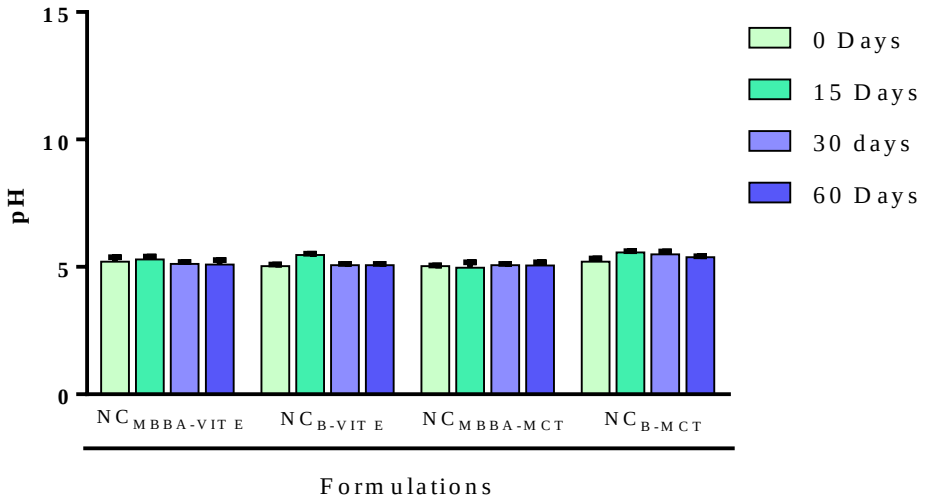

Figure 3ES:

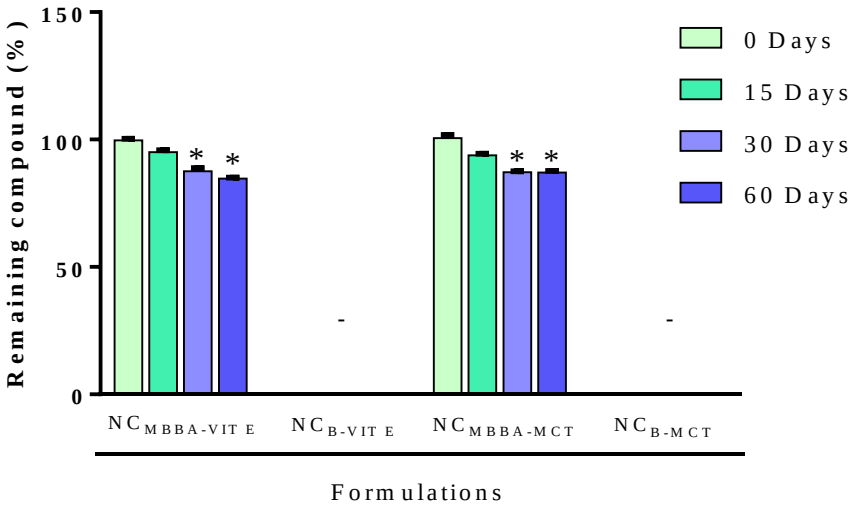

Figure 3S: Stability evaluation of the MBBA-loaded nanocapsule suspensions ($NC_{MBBA\text{-}VIT\ E}$ and $NC_{MBBA\text{-}MCT}$) and their respective unloaded (blank) formulations ($NC_{B\text{-}VIT\ E}$ and $NC_{B\text{-}MCT}$) on days 0-60. (Size – Fig. 3SA; Polydispersity Index – Fig. 3SB; Zeta Potential – Fig.3SC; pH – Fig. 3SD and Remaining compound – Fig. 3SE). The values are reported as mean ± S.E.M of 3/formulation. The data were analyzed using a Two-way ANOVA of repeated measures followed by the Tukey's test).

Figure 4AS:

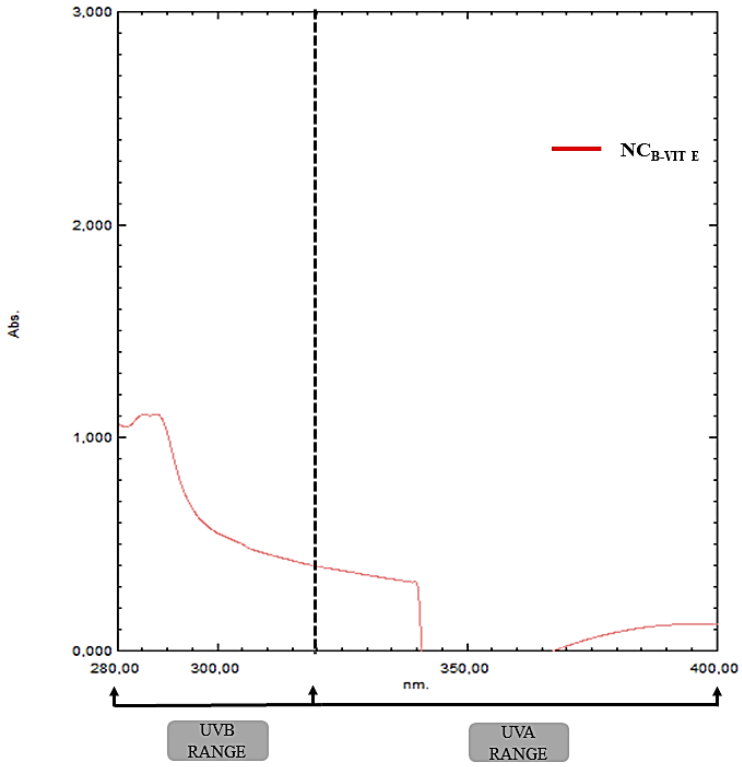

Figure 4BS:

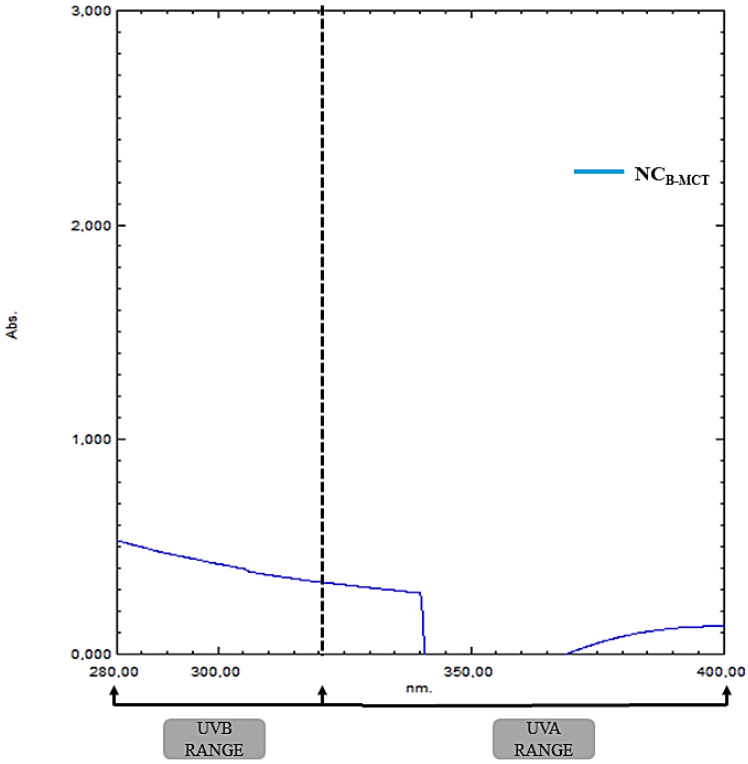

Figure 4S: *In vitro* UV light absorptive/scatter representative spectrum of the blank nanocapsules suspensions: $NC_{B\text{-}VIT\ E}$ (Fig. 4SA) and $NC_{B\text{-}MCT}$ (Fig.4SB).

4. CONCLUSÃO

O presente estudo demonstrou o potencial fotoprotetor do composto MBBA, uma inédita molécula pertencente à classe dos benzofuroazepinos. Corroborando com isso, propomos o emprego da nanotecnologia com o propósito de potencializar as propriedades de absorção do composto, bem como contornar limitações referentes a limitações no manejo farmacotécnico de formulações fotoprotetoras. Os resultados demonstraram que as suspensões de nanocápsulas foram desenvolvidas com sucesso, possuindo tamanho nanométrico adequado, propriedade mucoadesiva e fotoestabilidade. Além disso, os hidrogéis de base nanotecnológica contendo o composto MBBA apresentaram propriedades adequadas para a aplicação cutânea e foram eficazes na proteção do DNA contra danos causados pela radiação UV. No entanto, cabe ressaltar que este estudo foi conduzido utilizando uma abordagem *in vitro* e, portanto, mais estudos são necessários para determinar o potencial fotoprotetor dos hidrogéis.

5. REFERÊNCIAS

AKHALAYA, M. Y. et al. Molecular action mechanisms of solar infrared radiation and heat on human skin. **Ageing Research Reviews**, v. 16, n. 1, p. 1–11, 2014.

BAGDE, A.; MONDAL, A.; SINGH, M. Drug delivery strategies for chemoprevention of UVB-induced skin cancer: A review. **Photodermatology Photoimmunology and Photomedicine**, v. 34, n. 1, p. 60–68, 2018.

BROWNLOW, B. et al. Development and in Vitro Evaluation of Vitamin E-Enriched Nanoemulsion Vehicles Loaded with Genistein for Chemoprevention Against UVB-Induced Skin Damage. **Journal of Pharmaceutical Sciences**, v. 104, n. 10, p. 3510–3523, 2015.

CONTRI, R. V. et al. Skin penetration and dermal tolerability of acrylic nanocapsules: Influence of the surface charge and a chitosan gel used as vehicle. **International Journal of Pharmaceutics**, v. 507, n. 1–2, p. 12–20, 2016.

D'ORAZIO, J. et al. UV radiation and the skin. **International Journal of Molecular Sciences**, v. 14, n. 6, p. 12222–12248, 2013.

DAMERIS, M. Depletion of the ozone layer in the 21st century. **Angewandte Chemie - International Edition**, v. 49, n. 3, p. 489–491, 2010.

DELINASIOS, G. J. et al. Vitamin E inhibits the UVAI induction of "light" and "dark" cyclobutane pyrimidine dimers, and oxidatively generated DNA damage, in keratinocytes. **Scientific Reports**, v. 8, n. 1, p. 1–12, 2018.

FRANK, L. A. et al. Improving drug biological effects by encapsulation into polymeric nanocapsules. **Wiley Interdisciplinary Reviews: Nanomedicine and Nanobiotechnology**, v. 7, n. 5, p. 623–639, 2015.

FRANK, L. A. et al. Mucoadhesive Properties of Eudragit®RS100, Eudragit®S100, and Poly(ε-caprolactone) Nanocapsules: Influence of the Vehicle and the Mucosal Surface. **AAPS PharmSciTech**, v. 19, n. 4, p. 1637–1646, 2018.

GAI, R.; BACK, D. F.; ZENI, G. Potassium tert-Butoxide-Catalyzed Synthesis of Benzofuroazepines via Cyclization of (2-Alkynylbenzyl)oxy Nitriles. **Journal of Organic Chemistry**, v. 80, n. 20, p. 10278–10287, 2015.

GUTERRES, S. S.; ALVES, M. P.; POHLMANN, A. R. Polymeric Nanoparticles, Nanospheres and Nanocapsules, for Cutaneous Applications. **Drug Target Insights**, v. 2, p. 117739280700200, 2007.

HAYDEN, C. G. J.; ROBERTS, M. S.; BENSON, H. A. E. Systemic absorption of sunscreen after topical application Nocturnal cough in patients with sputum production. **The Lancet**, v. 350, n. 9081, p. 863–864, 1997.

JIMÉNEZ, M. M. et al. Influence of encapsulation on the in vitro percutaneous absorption of octyl methoxycinnamate. **International Journal of Pharmaceutics**, v. 272, n. 1–2, p. 45–55, 2004.

JOSE, J.; NETTO, G. Role of solid lipid nanoparticles as photoprotective agents in cosmetics. **Journal of Cosmetic Dermatology**, n. January, 2018.

KAMMEYER, A.; LUITEN, R. M. Oxidation events and skin aging. **Ageing Research Reviews**, v. 21, p. 16–29, 2015.

KHEZRI, K.; SAEEDI, M.; MALEKI DIZAJ, S. Application of nanoparticles in percutaneous delivery of active ingredients in cosmetic preparations. **Biomedicine and Pharmacotherapy**, v. 106, n. April, p. 1499–1505, 2018.

KRAUSE, M. et al. Sunscreens: Are they beneficial for health? An overview of endocrine disrupting properties of UV-filters. **International Journal of Andrology**, v. 35, n. 3, p. 424–436, 2012.

KUNISADA, M. et al. Hydrochlorothiazide enhances UVA-induced DNA damage. **Photochemistry and Photobiology**, v. 89, n. 3, p. 649–654, 2013.

LIEBEL, F. et al. Irradiation of skin with visible light induces reactive oxygen species and matrix-degrading enzymes. **Journal of Investigative Dermatology**, v. 132, n. 7, p. 1901–1907, 2012.

MANCUSO, J. B. et al. Sunscreens: An Update. **American Journal of Clinical Dermatology**, v. 18, n. 5, p. 643–650, 2017.

MARCHIORI, M. C. L. et al. Hydrogel containing silibinin-loaded pomegranate oil based nanocapsules exhibits anti-inflammatory effects on skin damage UVB radiation-induced in mice. **Journal of Photochemistry and Photobiology B: Biology**, v. 170, p. 25–32, 2017.

MATSUMURA, Y.; ANANTHASWAMY, H. N. Toxic effects of ultraviolet radiation on the skin. **Toxicology and Applied Pharmacology**, v. 195, n. 3, p. 298–308, 2004.

MILESI, S. S.; GUTERRES, S. . Fatores determinantes da eficácia de fotoprotetores. **Caderno de Farmácia**, v. 18, n. 2, p. 81–87, 2002.

MOURET, S. et al. Assessment of the photoprotection properties of sunscreens by chromatographic measurement of DNA damage in skin explants. **Photochemistry and Photobiology**, v. 87, n. 1, p. 109–116, 2011.

NATARAJAN, V. T. et al. Multifaceted pathways protect human skin from UV radiation. **Nature Chemical Biology**, v. 10, n. 7, p. 542–551, 2014.

NOGUEIRA, C. W.; ROCHA, J. B. T. Toxicology and pharmacology of selenium: emphasis on synthetic organoselenium compounds. **Archives of Toxicology**, v. 85, n. 11, p. 1313–1359, 1 nov. 2011.

NOGUEIRA, C. W.; ZENI, G.; ROCHA, J. B. T. Organoselenium and organotellurium compounds: Toxicology and pharmacology. **Chemical Reviews**, v. 104, n. 12, p. 6255–6285, 2004.

OLIVEIRA, C. P. et al. An algorithm to determine the mechanism of drug distribution in lipid-core nanocapsule formulations. **Soft Matter**, v. 9, n. 4, p. 1141–1150, 2013.

PEGORARO, N. S. et al. Nanoencapsulation of coenzyme Q10 and vitamin E acetate protects against UVB radiation-induced skin injury in mice. **Colloids and Surfaces B: Biointerfaces**, v. 150, p. 32–40, 2017.

PROW, T. W. et al. Nanoparticles and microparticles for skin drug delivery. **Advanced Drug Delivery Reviews**, v. 63, n. 6, p. 470–491, 2011.

QUAN, T. et al. Matrix-degrading metalloproteinases in photoaging. **Journal of Investigative Dermatology Symposium Proceedings**, v. 14, n. 1, p. 20–24, 2009.

SCHUCH, A. P. et al. DNA damage as a biological sensor for environmental sunlight. **Photochemical and Photobiological Sciences**, v. 12, n. 8, p. 1259–1272, 2013.

SCHUCH, A. P. et al. Sunlight damage to cellular DNA: Focus on oxidatively generated lesions. **Free Radical Biology and Medicine**, v. 107, n. September 2016, p. 110–124, 2017.

SHAATH, N. A. Ultraviolet filters. **Photochemical and Photobiological Sciences**, v. 9, n. 4, p. 464–469, 2010.

SINGER, S.; KARRER, S.; BERNEBURG, M. Modern sun protection. **Current Opinion in Pharmacology**, v. 46, p. 24–28, 2019.

STENGEL, F. Homeostasis in Topical Photoprotection: Getting the Spectral Balance Right. **American journal of clinical dermatology**, v. 19, n. s1, p. 40–44, 2018.

STIEFEL, C.; SCHWACK, W. Photoprotection in changing times - UV filter efficacy and safety, sensitization processes and regulatory aspects. **International Journal of Cosmetic Science**, v. 37, n. 1, p. 2–30, 2015.

WANG, P. W. et al. Red Raspberry Extract Protects the Skin against UVB-Induced Damage with Antioxidative and Anti-inflammatory Properties. **Oxidative medicine and cellular longevity**, v. 2019, p. 9529676, 2019.

YOUNG, A. R.; CLAVEAU, J.; ROSSI, A. B. Ultraviolet radiation and the skin: Photobiology and sunscreen photoprotection. **Journal of the American Academy of Dermatology**, v. 76, n. 3, p. S100–S109, 2017.

ZASTROW, L. et al. Leonhard Zastrow, Martina C. Meinke, Stephanie Albrecht, Alexa Patzelt, and Juergen Lademann 26. **Ultraviolet Light in Human Health, Diseases and Environment**, 2017.